

Rotors for Moving Frames in Projective Geometric Algebra

by

Zachary Charles Joseph Leger

A thesis
presented to the University of Waterloo
in fulfillment of the
thesis requirement for the degree of
Master of Mathematics
in
Computer Science

Waterloo, Ontario, Canada, 2025

© Zachary Charles Joseph Leger 2025

Author's Declaration

I hereby declare that I am the sole author of this thesis. This is a true copy of the thesis, including any required final revisions, as accepted by my examiners.

I understand that my thesis may be made electronically available to the public.

Abstract

Projective Geometric Algebra (PGA) is a relatively new mathematical model to describe rigid-body motions. As such, there has yet to be in-depth research on using PGA in conjunction with differential geometry. In particular, PGA's ability to describe rigid-body motions appears to be well-suited to describe the instantaneous motion of moving frames associated with parametric curves. In this thesis, we derive rotors that perform the instantaneous motion of a parametric curve for the translation frame, Bishop frame and Frenet-Serret frame in 3 dimensions. We demonstrate the use of these rotors by iteratively applying them to the corners of a square to construct a square tube fitted around a helix. We also generalize the construction of the rotors associated with moving frames to an arbitrary number of dimensions. We thus further develop the use of PGA in the field of differential geometry.

Acknowledgements

This thesis could not have been made without the support of so many important people. First, I would like to thank my friends and family for all the support they have given me throughout my life. I would not be here if it weren't for them. I would like to thank my fiancée, Tiadora Ruza, for always supporting me. For the number of times I spoke to her about my work, it's fortunate she still enjoys the sound of my voice. I would also like to thank my supervisor, Stephen Mann, for his continued support throughout the writing of this thesis. His ongoing patience, frequent reviews and kindness have been invaluable to me. I wish you the best in your retirement.

Dedication

This is dedicated to Tiadora Ruza.
My future wife, my everything.
I'm so excited for what's to come.

Table of Contents

Author's Declaration	ii
Abstract	iii
Acknowledgements	iv
Dedication	v
List of Figures	ix
List of Tables	x
1 Introduction	1
2 Background	3
2.1 Homogeneous Coordinates	4
2.1.1 Points at Infinity	6
2.2 Tensor Algebra	7
2.3 Exterior Algebra	8
2.3.1 Elements Representative of Subspaces	9
2.3.2 Duality in the Exterior Algebra	10
2.3.3 The Antierior Product	12
2.3.4 Exomorphisms	14
2.4 Geometric Algebra	15
2.4.1 Transformations in Geometric Algebra	17

2.4.2	Composing Transformations Together	20
2.5	Projective Geometric Algebra	21
2.5.1	Dual Representation Justification	22
2.5.2	Lines and Planes	24
2.5.3	Duals of Lines and Planes	26
2.5.4	Euclidean Dual and Cross Product	27
2.6	The Translation Frame, The Bishop Frame and Frenet-Serret Frame	27
2.6.1	The Translation Frame	28
2.6.2	The Bishop Frame	28
2.6.3	The Frenet-Serret Frame and Darboux Vector	29
2.7	Related Work	31
3	Local Motion Rotors	34
3.1	Definitions	35
3.2	Translation Frame	36
3.3	Translation Frame Example	37
4	Second Order Local Motion Rotors	39
4.1	Constraints on $f(s)$	39
4.2	Bishop Frame	40
4.2.1	3D Bishop Frame via the Frenet-Serret Formulas	40
4.2.2	Bishop Frame in terms of f and \mathbf{T}	42
4.2.3	Bishop Frame Example	44
4.3	The Frenet-Serret Frame	45
4.3.1	Frenet-Serret Frame Example	46
4.4	Comparison of the Three Frames	48
4.4.1	Frenet-Serret Frame at Zero Curvature	48
4.5	Non-Arc Length Parameterized Curves	52
5	Higher Dimensional Frames	53
5.1	Translation Frames and Bishop Frames	53
5.2	Frenet-Serret Frames	53
5.3	The Darboux Bivector	56

6	Conclusions	57
6.1	Contributions	57
6.2	Future Directions	59
	References	61
	APPENDICES	63
A	Proof of $(\underline{\ell})^2 = -1$	64
B	Full Derivation of Frenet Frame Example Rotor	66
C	Full Derivation of Bishop Frame Example Rotor	67
D	Comparison of Notations	69

List of Figures

1.1	A square tube fitted around a helix.	2
2.1	2D homogeneous coordinates before and after a shearing operation.	5
2.2	Euclidean vector before and after a shearing operation.	6
2.3	A vector and its dual.	11
2.4	A demonstration of the antiexterior product	13
2.5	A depiction of the shear transformation being applied to direct representations of points in PGA.	23
2.6	A depiction of an offset line in PGA.	25
2.7	A depiction of the osculating circle.	29
2.8	A depiction of the moving osculating plane in the Frenet-Serret frame.	30
2.9	A depiction of the components of a Darboux vector.	31
3.1	A depiction of a screw motion.	35
3.2	A comparison of first degree LMRs and second degree LMRs.	37
3.3	A depiction of the translation frame on $f(t) = t\mathbf{e}_1 + (t^2 + t)\mathbf{e}_2 + \mathbf{e}_0$	38
4.1	A depiction of the line intersecting the osculating circle's center.	41
4.2	The Bishop frame on a cubic Bézier curve.	44
4.3	A comparison of basis vectors for the translation frame, the Bishop frame and the Frenet-Serret frame.	49
4.4	A comparison of tubes for the translation frame, the Bishop frame and the Frenet-Serret frame.	50
4.5	The Frenet-Serret frame on a cubic Bézier curve.	51

List of Tables

2.1	Basis elements of a 3D exterior algebra	10
2.2	Value of \mathbf{e}_{ij}^2 for various signatures.	18
2.3	A table of blades and their corresponding direct and dual representations for 3D PGA.	26
2.4	A table of functions for the Frenet-Serret frame for the function f_\bullet	30
D.1	A table comparing the notation of this thesis, Dorst and De Keninck, and Lengyel.	69

Chapter 1

Introduction

The ability to model rigid-body motions is crucial to many applications, including robotics, computer graphics, and physics. Thus, there is considerable motivation to succinctly describe rigid-body motions mathematically. Geometric algebra is known for its ability to generalize quaternions, and in particular, the ability to describe rotations in a quaternion-like way for an arbitrary number of dimensions. Hence, geometric algebra is a desirable tool to describe rigid-body transformations, which are compositions of rotations and translations. However, for an n -dimensional space, an n -dimensional geometric algebra is unable to perform translation via multiplication, and thus cannot model rigid-body transformations via multiplication. The relatively new model of Projective Geometric Algebra (PGA) is a combination of homogeneous coordinates and geometric algebra. The homogeneous coordinate system allows the algebra to perform translation in addition to rotation via multiplication. In PGA, elements called *rotors* are the elements that correspond to rigid-body transformations.

In the interest of simulating real-world objects, one may want to model a rigid body following the path of a curve. Models of rigid body movements have applications in computer graphics. For example, an animator may want to have a character follow a particular path, or an artist may want to create a tube around a curve. See Figure 1.1 for an illustration of a square tube fitted around a helix. We describe paths using parametric curves, that is, curves defined via functions of the form $f : \mathbb{R} \rightarrow \mathbb{R}^n$, that map time (or arc length) to a vector indicating a position in the vector space.

A *frame* is a data structure containing a point of origin and unit orthogonal basis vectors. A change of the point of origin corresponds to a translation, and a change of basis vectors corresponds to a rotation. By beginning with an arbitrarily chosen frame and describing how the frame moves in time, we are able to describe rigid-body motions.

Given a parametric curve, there are infinitely many possible rigid-body motions that follow the path of the curve. In particular, requiring the rigid-body motion to follow the

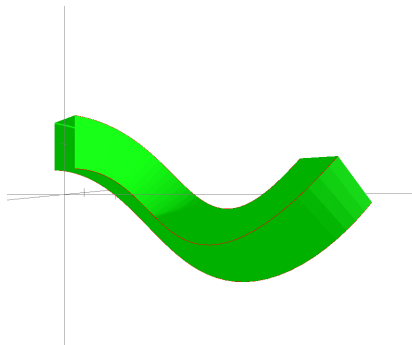


Figure 1.1: A square tube fitted around a helix.

path of the curve only restricts the frame's origin. Hence, given a fixed arbitrary starting frame, there are infinitely many ways in which the frame can transform over time. However, certain frames are of particular interest. In this thesis, we concern ourselves with the *translation frame*, the *Bishop frame* and the *Frenet-Serret frame*.

We are motivated by the following question: given a parametric curve and an associated frame, can we construct a rotor that describes the motion of the frame at a particular moment in time? And in particular, how can we do so using PGA?

In the second chapter, we provide the required background to understand the results of this thesis. In particular, we describe PGA and the frames associated with parametric curves. The chapter concludes with a section on related work. In the third chapter, we define Local Motion Rotors and show how to construct rotors for the simplest frame, the translation frame. In the fourth chapter, we cover Second Order Local Motion Rotors to create rotors associated with the Bishop frame and Frenet-Serret frame. As an example, we compute a square tube fitted around a helix by iteratively applying the rotors for each variety of moving frame. In the fifth chapter, we show how the rotors for the translation frame, Bishop frame and Frenet-Serret frame generalize to higher-dimensional spaces. The sixth chapter concludes the thesis with a comparison to the standard methods and a discussion on future extensions and variations of the approach developed in this thesis.

Chapter 2

Background

The purpose of this thesis is to combine the mathematical tooling of PGA with the techniques of moving frames for parametric curves in differential geometry. Thus, one must have a grasp of both to understand this thesis. In this chapter, we provide an explanation of homogeneous coordinates and a brief overview of PGA. See Dorst et al. [17] for more details on geometric algebra. For more details on PGA, see Dorst and De Keninck [6] or Lengyel [16]. In Section 2.6 we cover moving frames associated with parametric curves. For more details on such moving frames, see Nutbourne and Martin [20].

The fundamental transformation operation in geometric algebra is the application of a sandwiching operation, of the form

$$VxV^{-1}$$

where V is an invertible element we call a *versor* and x is a vector. A *rotor* is a particular type of versor that does not allow for the reflection operation. Compare this method of transformation to traditional linear algebra, where we have

$$Mx$$

where M is a matrix. In both geometric algebra and linear algebra, when $x = 0$, the transformation operation results in 0. Hence, the origin cannot be transformed to any other position in either algebra through their standard transformation methods. Of course, translation can be performed via addition in both geometric and linear algebra. However, there is considerable motivation (including mathematical simplifications and computational efficiency) to combine Euclidean rigid-body transformations (rotations and translation) into one mathematical element. The standard linear algebra approach is to use homogeneous coordinates, discussed in Section 2.1.

To understand geometric algebra, it is useful to understand the tensor algebra, and imperative to understand the exterior algebra. We cover the tensor algebra in Section 2.2 and

the exterior algebra in Section 2.3. We then describe geometric algebra in Section 2.4. Once an understanding of geometric algebra is established, we explain PGA as the combination of the homogeneous coordinate system and geometric algebra in Section 2.5.

Additionally, we cover the techniques of differential geometry for associating moving frames with parametric curves in Section 2.6.

2.1 Homogeneous Coordinates

In the homogeneous coordinates model of linear algebra, an n -dimensional space is extended by adding an extra axis, augmenting the space into an $(n + 1)$ -dimensional space. We will refer to this additional axis as the *projective axis* and denote it \mathbf{e}_0 . Additionally, we will refer to an n -tuple of real values as a *finite point* in the space. When an n -dimensional vector space is used to represent n -dimensional finite points, there is typically a direct correspondence between vectors and finite points

$$(v_1, v_2, \dots, v_n) \leftrightarrow \begin{bmatrix} v_1 \\ v_2 \\ \vdots \\ v_n \end{bmatrix}.$$

However, in the homogeneous model we assign all of the vectors representing *finite points* in our space the same value for the projective coordinate. Typically this value is 1. Thus we have

$$(v_1, v_2, \dots, v_n) \leftrightarrow \begin{bmatrix} v_1 \\ v_2 \\ \vdots \\ v_n \\ 1 \end{bmatrix}.$$

We refer to the hyperplane of vectors with value 1 in the projective axis as the *affine hyperplane*. See Figure 2.1 (a) for an illustration.

Thus, the point at position \vec{v} in \mathbb{R}^n will be represented by $\vec{v} + \mathbf{e}_0$ in the projective space \mathbb{R}^{n+1} . We say that the vector $\vec{v} + \mathbf{e}_0$ *represents* the finite point (v_1, v_2, \dots, v_n) .

Since all vectors representing finite points are offset from the origin, we can perform a transformation that will appear as translation when observing finite points. In particular, we will perform shear along the desired translation direction measured by the value in the projective coordinate. When discussing the shear operation, we will describe a shear as being *in the direction* v , where v simply indicates the direction of shear (with no regards to the magnitude of v). Additionally, we use the notation $[w]$ to extract the coefficient of

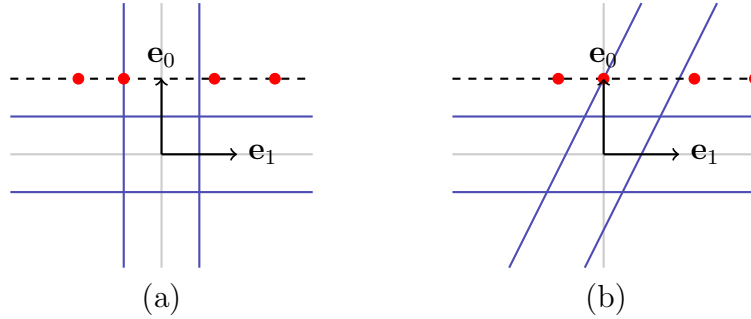


Figure 2.1: A Euclidean axis (\mathbf{e}_1) and a projective axis (\mathbf{e}_0). Red dots mark points in the scene. A dotted line denotes the affine hyperplane. (a) The scene before the shear transformation and (b) the scene after the shear transformation. The axis-aligned blue lines are tilted in (b) to show the effects of shear.

the w term of a vector. For example, if $v = \alpha w + c$ for some vector c orthogonal to w , then $[w]v = \alpha$. We say that a shear transformation is *measured by* $\beta[w]$, if the transformation moves the vector v by $\beta[w]v$ for all v in the vector space. For example, the matrix

$$\begin{bmatrix} 1 & 2 \\ 0 & 1 \end{bmatrix}$$

corresponds to a shear in direction \mathbf{e}_1 measured by $2[\mathbf{e}_2]$. If we apply the transformation to the vector $v = [7 \ 3]^T$ we get

$$\begin{bmatrix} 1 & 2 \\ 0 & 1 \end{bmatrix} \begin{bmatrix} 7 \\ 3 \end{bmatrix} = \begin{bmatrix} 7 + 2 \cdot 3 \\ 3 \end{bmatrix}$$

which corresponds to moving the vector in the direction \mathbf{e}_1 by the amount of 2 times the coefficient of the \mathbf{e}_2 value of $[7 \ 3]^T$.

Since all vectors representing finite points have value 1 in the projective coordinate, we can mimic translation by distance $\alpha \in \mathbb{R}$ in the affine hyperplane by performing shear in the desired Euclidean direction \vec{v} measured by $\alpha[\mathbf{e}_0]$. See Figure 2.1 for an illustration of how the shear transformation mimics translation in the homogeneous model. Thus, by extending the space by an extra dimension and setting the projective coordinate to 1, we are able to perform a linear transformation that mimics translation. Since shearing is a linear transformation, it can be performed via a matrix. Furthermore, all linear transformations that are restricted to the Euclidean axes (namely rotations) perform identically in the extended space. Thus, by using homogeneous coordinates we are able to perform any rigid-body transformation using a series of matrices. Since a series of matrices can be combined into a single matrix, we are thus able to represent any rigid body transformation via a single matrix.

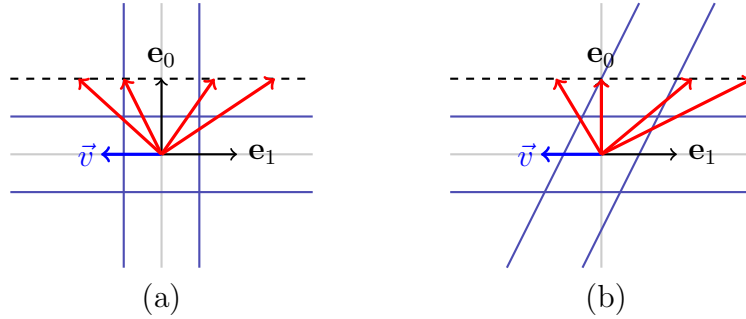


Figure 2.2: A Euclidean axis (\mathbf{e}_1) and a projective axis (\mathbf{e}_0). A blue Euclidean vector \vec{v} pointing left. Red arrows mark the vectors representing points in the scene. A dotted line denotes the affine hyperplane. (a) The scene before the shear transformation and (b) the scene after the shear transformation. The axis-aligned blue lines are tilted in (b) to show the effects of shear. Notice that the transformation does not change the Euclidean vector \vec{v} .

2.1.1 Points at Infinity

The addition of the projective axis allows for the creation of elements beyond those of the form $p = \vec{v} + \mathbf{e}_0$ where \vec{v} is an element in the original n -dimensional space. Since the shear transformation preserves lines extending from the origin, we can consider every vector that intersects the affine hyperplane at $\vec{v} + \mathbf{e}_0$ as representing the finite point (v_1, \dots, v_n) as well. In essence, we have an equivalence relation \sim where $A \sim B$ if and only if $A = \alpha B$ for some scalar α . Hence, all vectors of the form $\alpha(\vec{v} + \mathbf{e}_0)$ for some $\alpha \in \mathbb{R}$ represent the finite point (v_1, \dots, v_n) . Therefore, we are able to interpret every vector with a non-zero \mathbf{e}_0 coefficient as having the geometric interpretation of a finite point.

However, not all vectors in \mathbb{R}^{n+1} can be rescaled such that the coefficient of the \mathbf{e}_0 component will be 1. In particular, vectors with a value of 0 in the projective axis, that is, vectors of the form

$$[v_1 \ v_2 \ \dots \ v_n \ 0]^T,$$

cannot be rescaled to modify the \mathbf{e}_0 component. We refer to vectors with a 0 value in the projective axis as *Euclidean vectors* and denote such vectors with an arrow above the vector element, for example \vec{v} . Notice that every Euclidean vector \vec{v} is parallel to the affine hyperplane. Also notice that the Euclidean vector \vec{v} will transform under the rotation transformations of the Euclidean space but will *not* transform under the shear transformation. See Figure 2.2 for an illustration of Euclidean vectors not transforming under the shear operation. Thus, a geometric interpretation of these vectors is to view them as *points at infinity*, since they are transformed by rotation but not shear (which corresponds to translation). Just like finite points, rescaling the vector \vec{v} does not change the point it represents. We collectively denote the set of finite points and points at infinity as *points*. Under this

interpretation, every vector represents a point, and rescaling the vector never changes its geometric interpretation.

However, it is worth noting that Euclidean vectors are not always interpreted as points at infinity. In particular, given two finite points lying on the affine hyperplane, say $\vec{v} + \mathbf{e}_0$ and $\vec{w} + \mathbf{e}_0$, the difference between them is a Euclidean vector $\vec{v} - \vec{w}$. This Euclidean vector can be viewed as having the geometric interpretation of a *direction with magnitude* pointing from one point to the other, rather than a point at infinity. The distinction is that the geometric interpretation of a direction with magnitude *does* change upon scaling the element by a scalar. These two geometric interpretations can be used for the same Euclidean vector depending on the context. Vectors and directions with magnitude are often used synonymously (i.e., vectors are seen as arrows with a certain length), however in this thesis we strictly use the term *vector* to mean elements of the vector space (linear combination of basis vectors) that are not necessarily Euclidean. Directions with magnitude are always referred to as Euclidean vectors.

2.2 Tensor Algebra

The tensor algebra of $V = \mathbb{R}^n$ is the algebra of elements created from vectors in V and the operations of addition and the tensor product, denoted \otimes . The tensor product is a bilinear product, that is to say, it has the properties

$$\begin{aligned} a \otimes (b + c) &= a \otimes b + a \otimes c \\ (a + b) \otimes c &= a \otimes c + b \otimes c \\ (\alpha a) \otimes b &= a \otimes (\alpha b) = \alpha(a \otimes b) \end{aligned}$$

for all $a, b \in V$ and $\alpha \in \mathbb{R}$. The tensor product is by definition associative. Thus, if we are given two vector spaces W_1 and W_2 with standard bases B_{W_1} and B_{W_2} , the tensor product has the property that for all vectors of the form

$$\begin{aligned} x_1 &= \sum_{w_1 \in B_{W_1}} \alpha_{w_1} w_1 \\ x_2 &= \sum_{w_2 \in B_{W_2}} \alpha_{w_2} w_2 \end{aligned}$$

then we have the equality

$$x_1 \otimes x_2 = \sum_{w_1 \in B_{W_1}, w_2 \in B_{W_2}} \alpha_{w_1} \alpha_{w_2} (w_1 \otimes w_2).$$

Thus, it suffices to consider the effects of $w_1 \otimes w_2$ for the basis elements of W_1 and W_2 [8]. We presuppose that we are given a standard basis $\mathbf{e}_1, \mathbf{e}_2, \dots, \mathbf{e}_n$ for \mathbb{R}^n . As an example, the tensor product between $\mathbf{e}_1 + \mathbf{e}_2$ and $\mathbf{e}_1 + 2\mathbf{e}_3$ is

$$(\mathbf{e}_1 + \mathbf{e}_2) \otimes (\mathbf{e}_1 + 2\mathbf{e}_3) = \mathbf{e}_1 \otimes \mathbf{e}_1 + 2\mathbf{e}_1 \otimes \mathbf{e}_3 + \mathbf{e}_2 \otimes \mathbf{e}_1 + 2\mathbf{e}_2 \otimes \mathbf{e}_3$$

and the tensor product between $\mathbf{e}_1 \otimes \mathbf{e}_2$ and $\mathbf{e}_1 + \mathbf{e}_3$ is

$$(\mathbf{e}_1 \otimes \mathbf{e}_2) \otimes (\mathbf{e}_1 + \mathbf{e}_3) = \mathbf{e}_1 \otimes \mathbf{e}_2 \otimes \mathbf{e}_1 + \mathbf{e}_1 \otimes \mathbf{e}_2 \otimes \mathbf{e}_3.$$

In the tensor algebra, every element of the form $\mathbf{e}_{i_1} \otimes \mathbf{e}_{i_2} \otimes \dots \otimes \mathbf{e}_{i_k}$ for some symbols $i_1, \dots, i_k \in [1, n]$ are valid and distinct elements of the algebra. Hence, the tensor algebra of $V = \mathbb{R}^n$ can be viewed as the algebra of polynomials over n non-commutative variables [14].

The tensor product results in a *graded algebra*. This means that there is a natural grading that can be assigned to elements formed from basis vectors and the tensor product. We say that an element where every term has k symbols is of grade k . This property is thus closed under addition. Furthermore, the grading has the property that for any grade k element E_k and any grade l element E_l , the grade of $E_k \otimes E_l$ is $k + l$. For example, the grade of $\mathbf{e}_1 \otimes \mathbf{e}_2$ is 2 and the grade of $\mathbf{e}_1 + \mathbf{e}_3$ is 1. Thus, the grade of $\mathbf{e}_1 \otimes \mathbf{e}_2 \otimes \mathbf{e}_3$ is 3. Not all elements in the algebra can be assigned a grade. For example, the elements $\mathbf{e}_1 + \mathbf{e}_1 \otimes \mathbf{e}_2$ and $1 + \mathbf{e}_1$ are of mixed grade.

We denote the space of elements of grade k as $T^k(V)$ and the entire tensor algebra space as $T(V)$. Given a basis $\{\mathbf{e}_1, \mathbf{e}_2, \dots, \mathbf{e}_n\}$ for the vector space $V = \mathbb{R}^n$, there is a natural extension to which we can create a vector space for $T(V)$. In particular, every element in $T(V)$ is a linear combination of the elements

$$\{1, \mathbf{e}_1, \mathbf{e}_2, \dots, \mathbf{e}_n, \mathbf{e}_1 \otimes \mathbf{e}_1, \mathbf{e}_1 \otimes \mathbf{e}_2, \dots, \mathbf{e}_n \otimes \mathbf{e}_n, \mathbf{e}_1 \otimes \mathbf{e}_1 \otimes \mathbf{e}_1, \dots\}. \quad (2.1)$$

We will refer to the set $\{\mathbf{e}_1, \mathbf{e}_2, \dots, \mathbf{e}_n\}$ as the basis of the vector space and the set in Equation 2.1 as the basis of the algebra. Note that the basis of the tensor algebra is infinitely large; this is not the case for the exterior or geometric algebras. Furthermore, note that in the tensor algebra, $a \otimes b$ is a distinct element from $b \otimes a$ (they bear no relation to one another). This also differs from the exterior and geometric algebras.

2.3 Exterior Algebra

We consider the exterior algebra of V as the space of elements

$$\bigwedge(V) := \frac{T(V)}{\{v \otimes v : v \in V\}}. \quad (2.2)$$

That is to say, we set $v \otimes v \equiv 0$ for all elements $v \in V$. The result is also an algebra with an associative and bilinear product. We refer to this product as the *exterior product* (it is also called the *outer product* or *wedge product*) and denote it \wedge .

For brevity of notation, we let $\mathbf{e}_I \wedge \mathbf{e}_J = \mathbf{e}_{IJ}$ for any symbols I and J . Since the exterior product is associative, we have

$$\mathbf{e}_{IJ} \wedge \mathbf{e}_K = (\mathbf{e}_I \wedge \mathbf{e}_J) \wedge \mathbf{e}_K = \mathbf{e}_I \wedge (\mathbf{e}_J \wedge \mathbf{e}_K) = \mathbf{e}_I \wedge \mathbf{e}_{JK}.$$

Thus, both results can be unambiguously written as \mathbf{e}_{IJK} .

By the quotient in Equation 2.2, the fundamental property of the exterior product is that for all vectors v , we have $v \wedge v = 0$, which implies that $\mathbf{e}_{ij} = -\mathbf{e}_{ji}$ since

$$0 = (\mathbf{e}_i + \mathbf{e}_j) \wedge (\mathbf{e}_i + \mathbf{e}_j) = \mathbf{e}_i \wedge \mathbf{e}_i + \mathbf{e}_{ij} + \mathbf{e}_{ji} + \mathbf{e}_j \wedge \mathbf{e}_j = \mathbf{e}_{ij} + \mathbf{e}_{ji}.$$

Additionally, all elements with duplicated subscripts are 0. For example,

$$\mathbf{e}_{121} = -\mathbf{e}_{112} = -(\mathbf{e}_1 \wedge \mathbf{e}_1) \wedge \mathbf{e}_2 = 0 \wedge \mathbf{e}_2 = 0.$$

The exterior algebra still retains the grading of the tensor algebra. A grade k element of the exterior algebra is referred to as a k -vector. For example, the element $\mathbf{e}_{123} + \mathbf{e}_{345}$ is a 3-vector and the element \mathbf{e}_1 is a 1-vector. 1-vectors are vectors and are usually referred to as such. The terms *bivector* to mean 2-vector and *trivector* to mean 3-vector are also commonly used. The exterior algebra also retains mixed grade elements. For example, the element $1 + \mathbf{e}_1$ is a mixed grade element.

2.3.1 Elements Representative of Subspaces

The exterior algebra gains an extra feature compared to the tensor algebra: elements of the form

$$v_1 \wedge v_2 \wedge \dots \wedge v_k$$

can be viewed as representative of a k -dimensional linear subspace. We call elements that can be written in this form as *decomposable k -vectors* or simply *k -blades*. If v_1, \dots, v_k are linearly independent vectors, then the k -blade $v_1 \wedge \dots \wedge v_k$ represents the subspace spanned by v_1, \dots, v_k . If the vectors v_1, \dots, v_k are not linearly independent, then the exterior product operations will yield the zero element. Non-zero scalars are 0-blades and vectors are 1-blades by definition.

The reason that we can view certain elements in the exterior algebra as representative of linear subspaces is that the elements are tied to the linear dependence of the multiplicands. In particular, we have the relation

$$v_1 \wedge v_2 \wedge \dots \wedge v_k = 0 \iff v_1, \dots, v_k \text{ are linearly dependent}$$

Grade	Basis Elements
0	1
1	$\mathbf{e}_1, \mathbf{e}_2, \mathbf{e}_3$
2	$\mathbf{e}_{12}, \mathbf{e}_{13}, \mathbf{e}_{23}$
3	\mathbf{e}_{123}

Table 2.1: Basis elements of a 3-dimensional exterior algebra with basis vectors $\mathbf{e}_1, \mathbf{e}_2$ and \mathbf{e}_3 , categorized by grade.

Hence, we can view k -blades as being representative of a k -dimensional linear subspaces, since if we have $E_k = v_1 \wedge v_2 \wedge \dots \wedge v_k$, then we have that $E_k \wedge w = 0$ if and only if w is in the linear subspace spanned by v_1, \dots, v_k .

Since $\mathbf{e}_{ij} = -\mathbf{e}_{ji}$, we have that the permutation of subscripts does not result in new basis elements. For example, we have

$$\mathbf{e}_{123} = -\mathbf{e}_{132} = -\mathbf{e}_{213} = \mathbf{e}_{231} = \mathbf{e}_{312} = -\mathbf{e}_{321}.$$

Furthermore, in an n -dimensional space, a set of $n + 1$ vectors must always be linearly dependent. Hence, all $(n + 1)$ -blades or larger must collapse to 0. Thus, an n -dimensional exterior algebra has a limited number of basis elements. In particular, there will be $\binom{n}{k}$ basis elements of grade k for $0 \leq k \leq n$, and there will be 2^n basis elements in total. For example, the elements of a 3D space are given in Table 2.1.

2.3.2 Duality in the Exterior Algebra

There is significant *geometric* motivation for defining dual operations in the exterior algebra. Recall that in an n -dimensional space, a grade k element represents a k -dimensional linear subspace. There is thus an $(n - k)$ -dimensional linear subspace perpendicular to it. A corresponding dual element can represent this perpendicular subspace. See Figure 2.3 for an illustration of a linear subspace and its dual.

Furthermore, notice that there is a symmetry in the number of basis elements of each grade in the exterior algebra. In particular,

$$\#\text{basis elements of grade } k = \binom{n}{k} = \binom{n}{n-k} = \#\text{basis elements of grade } n - k$$

Hence, given a set of basis vectors, there is a natural inclination to create a mapping between k -vectors and $(n - k)$ -vectors. There are infinitely many such mappings. Lengyel provides a mapping called the *left and right complement* [16]. In an n -dimensional space with basis vectors $\mathbf{e}_1, \mathbf{e}_2, \dots, \mathbf{e}_n$, the largest grade basis element is $\mathbf{e}_{123\dots n}$. We refer to this element as

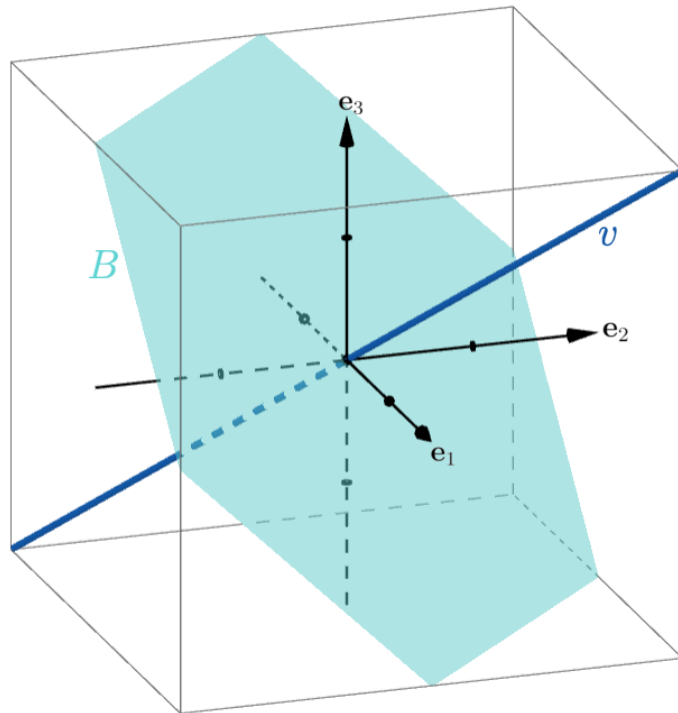


Figure 2.3: The vector $v = \mathbf{e}_1 + \mathbf{e}_2 + \mathbf{e}_3$ and its dual $B = \mathbf{e}_{23} - \mathbf{e}_{13} + \mathbf{e}_{12}$. The vector v is illustrated by a dark blue line and the bivector B is illustrated by a light blue plane.

the *pseudoscalar* and denote it $\mathbb{1}$. For each k -blade $E_k = \mathbf{e}_{i_1} \wedge \mathbf{e}_{i_2} \wedge \dots \wedge \mathbf{e}_{i_k}$ of the basis elements, the left complement of E_k is denoted \underline{E}_k is the unique $(n - k)$ -blade such that

$$\underline{E}_k \wedge E_k = \mathbb{1}.$$

The right complement is denoted \overline{E}_k and denotes the unique $(n - k)$ -blade such that

$$E_k \wedge \overline{E}_k = \mathbb{1}.$$

The left and right complements are equivalent to each other up to sign. In particular, the sign difference is

$$\overline{E}_k = (-1)^{k(n-k)} \underline{E}_k.$$

These mappings are linear, and thus it suffices to apply them to each basis element. For example,

$$\overline{\mathbb{1} + 2\mathbf{e}_1 + 3\mathbf{e}_{12}} = \overline{\mathbb{1}} + 2\overline{\mathbf{e}_1} + 3\overline{\mathbf{e}_{12}} = \mathbb{1} + 2\mathbf{e}_{23\dots n} + 3\mathbf{e}_{34\dots n}.$$

The left and right complements are inverses of each other. Thus, for any element E we have $\overline{\underline{E}} = E$. The complements of the zero element is 0

$$\overline{0} = \underline{0} = 0.$$

The left and right complement operations closely resemble the Hodge dual operator \star commonly used in exterior algebra literature. Their relation to one another is detailed in Appendix D.

We note that the complement of a vector is referred to as a *pseudovector*. For example, in 3D, we have the pseudovectors $\underline{\mathbf{e}}_1 = \mathbf{e}_{23}$, $\underline{\mathbf{e}}_2 = -\mathbf{e}_{13}$ and $\underline{\mathbf{e}}_3 = \mathbf{e}_{12}$.

2.3.3 The Antierior Product

We have seen that given a k -blade E_k and a vector v that is linearly independent from the subspace of E_k , computing $E_{k+1} := E_k \wedge v$ creates an element that represents a $(k + 1)$ -dimensional subspace. In essence, the exterior product increases the dimension of the subspace. It is also desirable to have an operation that is able to *reduce* the dimensionality of the represented subspace. From the dual perspective, decreasing the dimensionality of an element is equivalent to increasing the dimensionality of the dual element.

We define an operation \vee such that for all elements A and B ,

$$A \vee B := \overline{\underline{A} \wedge \underline{B}} = \overline{\underline{A} \wedge \underline{B}}.$$

We refer to the operation as the *antierior product*, though it is also called the *join*, *antiwedge product*, or *regressive product*. The operation performs intersections on linear

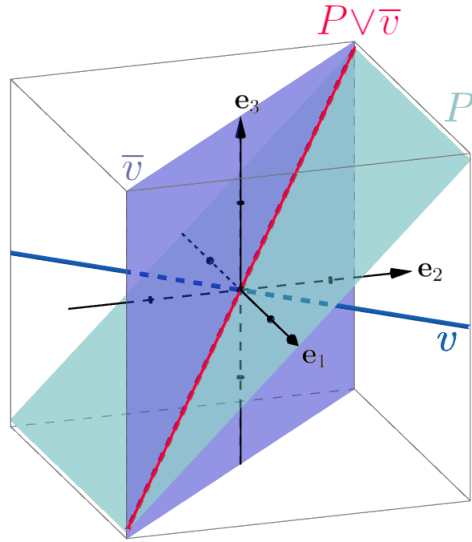


Figure 2.4: A demonstration of the antiexterior product. The light blue plane is the plane represented by $P = \mathbf{e}_1 \wedge (\mathbf{e}_2 + \mathbf{e}_3)$. The dark blue line is the line represented by $v = \mathbf{e}_1 + \mathbf{e}_2$ and the purple plane is the plane represented by $\bar{v} = \overline{\mathbf{e}_1 + \mathbf{e}_2}$. The red line is the line represented by $P \vee \bar{v} = \mathbf{e}_2 + \mathbf{e}_3 - \mathbf{e}_1$ and lies at the intersection of the planes represented by P and \bar{v} .

subspaces if the span of any pair of multiplicands covers the entire vector space. Otherwise, the antiexterior product results in 0. For example, in a 3D vector space, given an element $P = \mathbf{e}_1 \wedge (\mathbf{e}_2 + \mathbf{e}_3)$ representing a 2D plane and the pseudovector $\bar{v} = \overline{\mathbf{e}_1 + \mathbf{e}_2}$, an element that represents the plane that is perpendicular to the vector $v = \mathbf{e}_1 + \mathbf{e}_2$, we can compute

$$\begin{aligned}
 P \vee \bar{v} &= \left(\mathbf{e}_1 \wedge (\mathbf{e}_2 + \mathbf{e}_3) \right) \vee \overline{\mathbf{e}_1 + \mathbf{e}_2} \\
 &= \overline{\left(\mathbf{e}_1 \wedge (\mathbf{e}_2 + \mathbf{e}_3) \right) \wedge (\mathbf{e}_1 + \mathbf{e}_2)} \\
 &= \overline{(\mathbf{e}_{12} + \mathbf{e}_{13}) \wedge (\mathbf{e}_1 + \mathbf{e}_2)} \\
 &= \overline{(\mathbf{e}_3 - \mathbf{e}_2) \wedge (\mathbf{e}_1 + \mathbf{e}_2)} \\
 &= \overline{\mathbf{e}_{31} - \mathbf{e}_{21} + \mathbf{e}_{32}} \\
 &= \mathbf{e}_2 + \mathbf{e}_3 - \mathbf{e}_1.
 \end{aligned}$$

The space spanned by $\mathbf{e}_2 + \mathbf{e}_3 - \mathbf{e}_1$ is a 1D linear subspace contained in the subspace represented by $\mathbf{e}_1 \wedge (\mathbf{e}_2 + \mathbf{e}_3)$ and perpendicular to $\mathbf{e}_1 + \mathbf{e}_2$. See Figure 2.4 for an illustration.

Suppose two multiplicands of the antiexterior product do not cover the entire vector space. For example, $A = \mathbf{e}_1$ and $B = \mathbf{e}_2$. Then in a 3D vector space, the vector \mathbf{e}_3 does not

belong to the space of both. Hence, \mathbf{e}_3 belongs to the span of their complements, and the exterior product on the complements will result in zero,

$$\begin{aligned} A \vee B &= \overline{\mathbf{e}_1 \wedge \mathbf{e}_2} \\ &= \overline{\mathbf{e}_{23} \wedge \mathbf{e}_{13}} \\ &= 0. \end{aligned}$$

In general, if the span of A and B does not cover the entire space, then there is a vector v that is orthogonal to both. The vector v will be a factor in both complements, and that will result in a value of 0 for the exterior product.

To summarize, given elements E_k and E_l , the exterior product $E_k \wedge E_l$ creates an element that represents a subspace of size $k + l$ that is the union of the subspaces of E_k and E_l or collapses to 0 if such a union does not create a subspace of the correct size (i.e., the component vectors are not linearly independent). Similarly, given elements E_{n-k} and E_{n-l} , the antiexterior product $E_{n-k} \vee E_{n-l}$ creates an element that represents a subspace of size $n - k - l$ that is the intersection of the subspaces of E_k and E_l or collapses to 0 if such an intersection does not create an element of the correct size (i.e., there exists a vector perpendicular to both E_{n-k} and E_{n-l}).

2.3.4 Exomorphisms

A transformation $T : \bigwedge(V) \rightarrow \bigwedge(V)$ is an *exomorphism* if T is linear and has the property that for any k -blade $v_1 \wedge \dots \wedge v_k$ we have

$$T(v_1 \wedge v_2 \wedge \dots \wedge v_k) = T(v_1) \wedge T(v_2) \wedge \dots \wedge T(v_k).$$

In essence, the transformation T distributes over addition and the exterior product. From a geometric point of view, the property of distributing over addition means that applying transformations on each coordinate point individually and combining the results is the same as applying the transformation to the entire vector. The property of distributing over the exterior product means that transformations on linear subspaces are equivalent to applying the transformations to their component vectors.

In this thesis, we implicitly extend the domain of all transformations $T : V \rightarrow V$ to their exomorphic transformations $T : \bigwedge(V) \rightarrow \bigwedge(V)$. We overload the symbol of the original transformation. In particular, given a linear transformation represented by the matrix M , we apply M to elements in the exterior algebra exomorphically. For example, given

$$M = \begin{bmatrix} 1 & 2 \\ 3 & 4 \end{bmatrix},$$

we apply M to $\mathbf{e}_1 \wedge \mathbf{e}_2$ by

$$\begin{aligned} M(\mathbf{e}_1 \wedge \mathbf{e}_2) &= (M\mathbf{e}_1) \wedge (M\mathbf{e}_2) \\ &= (\mathbf{e}_1 + 3\mathbf{e}_2) \wedge (2\mathbf{e}_1 + 4\mathbf{e}_2) \\ &= 4\mathbf{e}_{12} + 6\mathbf{e}_{21} \\ &= -2\mathbf{e}_{12}. \end{aligned}$$

Given a transformation M , it will be useful to consider the corresponding transformation in the dual space. In particular, the transformation M on vectors corresponds to the transformation $\text{adj}(M)^T$ on pseudovectors, where $\text{adj}(M)$ is the adjugate matrix [16]. Concretely, this results in

$$M\underline{E} = \underline{\text{adj}(M)^T E}.$$

If the matrix M is invertible then the adjugate has the property

$$\text{adj}(M) = \det(M)M^{-1}.$$

The exomorphisms we are concerned with in this thesis (which take the form of versors in geometric algebra) will be rotations and shear transformations and their compositions. Rotation and shear transformations are both invertible and have determinants of 1, and thus so do the compositions of these transformations. Hence, for invertible matrices M with determinant 1,

$$\text{adj}(M)^T = M^{-T}. \quad (2.3)$$

2.4 Geometric Algebra

Instead of mapping $v \otimes v$ to 0, we instead consider the case of mapping $v \otimes v$ to a (potentially non-zero) scalar. That is, we consider the algebra

$$\frac{T(V)}{\{v \otimes v - Q(v) : v \in V\}}$$

where $Q(v)$ maps v to a scalar in \mathbb{R} . We call the product of this algebra the *geometric product* and denote it via concatenation. Hence, we have $vv - Q(v) = 0$ for all vectors v . We define an orthogonal basis of the vector space of the geometric algebra to be a basis $\{\mathbf{e}_1, \mathbf{e}_2, \dots, \mathbf{e}_n\}$ such that $\mathbf{e}_i \mathbf{e}_j$ does not contain a scalar term. Therefore, given two basis vectors \mathbf{e}_i and \mathbf{e}_j , we have that

$$\begin{aligned} Q(\mathbf{e}_i + \mathbf{e}_j) &= (\mathbf{e}_i + \mathbf{e}_j)(\mathbf{e}_i + \mathbf{e}_j) \\ &= \mathbf{e}_i \mathbf{e}_i + \mathbf{e}_i \mathbf{e}_j + \mathbf{e}_j \mathbf{e}_i + \mathbf{e}_j \mathbf{e}_j \\ &= Q(\mathbf{e}_i) + \mathbf{e}_i \mathbf{e}_j + \mathbf{e}_j \mathbf{e}_i + Q(\mathbf{e}_j). \end{aligned}$$

Since the left-hand side must be a scalar, so must the right-hand side. The terms $\mathbf{e}_i\mathbf{e}_j$ and $\mathbf{e}_j\mathbf{e}_i$ do not contain scalar terms and hence

$$Q(\mathbf{e}_i + \mathbf{e}_j) = Q(\mathbf{e}_i) + Q(\mathbf{e}_j) \quad (2.4)$$

and

$$\mathbf{e}_i\mathbf{e}_j = -\mathbf{e}_j\mathbf{e}_i.$$

In essence, as with the exterior product, the geometric product is anticommutative over orthogonal basis vectors. We assume throughout this thesis that the basis vectors for the vector space of our geometric algebras are always orthogonal. As a result, for any vector v and w that are orthogonal to each other, we have $vw = -wv$.

It can also be shown that $Q(\alpha v) = \alpha^2 Q(v)$. Since the function Q distributes over addition of basis vectors, as in Equation 2.4, and scalars can be extracted via $Q(\alpha v) = \alpha^2 Q(v)$, it suffices to consider what the value of $Q(\mathbf{e}_i)$ is for each basis vector \mathbf{e}_i . Additionally, the geometric product inherits the bilinearity of the tensor product. Thus, we see that if $Q(v) \neq 0$ then

$$Q\left(\frac{v}{\sqrt{|Q(v)|}}\right) = \frac{v}{\sqrt{|Q(v)|}} \frac{v}{\sqrt{|Q(v)|}} = \frac{vv}{|Q(v)|} = \frac{Q(v)}{|Q(v)|} = \pm 1.$$

Thus, we can rescale our basis elements as desired to achieve $Q(\mathbf{e}_i) = 0, 1$ or -1 . Hence, it suffices to consider $Q(\mathbf{e}_i) = 0, 1$ or -1 as possible options for each basis element \mathbf{e}_i . We refer to the choice of 0, 1, or -1 for each basis element as the *signature* of the space. If we choose $Q(\mathbf{e}_i) = 1$ for every \mathbf{e}_i , then the space is purely Euclidean and we refer to the signature as *non-degenerate*. Otherwise, we refer to the signature as *degenerate* [17]. The choice of signature effectively assigns a metric to the space.

The geometric product often results in elements of mixed grade. For example, given the signature $Q(\mathbf{e}_1) = 1$, the geometric product between $\mathbf{e}_1 + \mathbf{e}_2$ and \mathbf{e}_1 is

$$(\mathbf{e}_1 + \mathbf{e}_2)\mathbf{e}_1 = 1 - \mathbf{e}_1\mathbf{e}_2.$$

Additionally, we note that the geometric product is neither commutative nor anticommutative. Consider when vectors v and w are not necessarily orthogonal, then we have

$$Q(v + w) = (v + w)(v + w) = vv + ww + vw + wv = Q(v) + Q(w) + wv + vw$$

and hence we have the equality

$$wv = -vw + (Q(v + w) - Q(v) - Q(w)).$$

In essence, commuting multiplicands comes at the cost of scaling by -1 and adding a scalar.

Since the geometric product distributes over addition and duplicate entries reduce to scalars, we see that the elements of the geometric algebra are elements with non-repeating subscripts, just like the exterior algebra. Since the space of possible elements in both algebras are the same, we often use the exterior product and geometric product together. We also use the subscript notation in geometric algebra, e.g., $\mathbf{e}_{ij} = \mathbf{e}_i \mathbf{e}_j = \mathbf{e}_i \wedge \mathbf{e}_j$. The exterior product is often used to construct elements that represent linear subspaces, and the geometric product is then used with these elements to perform geometric transformations. For example, we might have an operation on vectors b, c and unit vector a such as

$$a(b \wedge c)a,$$

which performs a geometric transformation (reflection of the plane $b \wedge c$ through the vector a). We detail how the geometric product produces rigid-body transformations in the following section, although we do not detail the reflection operation.

2.4.1 Transformations in Geometric Algebra

Geometric algebras are of interest because they enable the use of elements in the exterior algebra to perform geometric transformations. In particular, suppose we are given an element R such that R is invertible (i.e., there exists R^{-1} such that $RR^{-1} = 1$) and that each term of R is of even grade. Then for any element E , the operation

$$R E R^{-1}$$

is an exomorphism. Of particular interest are rotors of the form

$$\exp\left(\frac{\Delta}{2} B\right)$$

where Δ is a scalar and B is a bivector (not necessarily a 2-blade). Depending on the signature of the space and the components of B , this rotor will have differing effects. In particular, to understand the effects of rotors of this form, it suffices to understand the effects of the basis elements of the form \mathbf{e}_{ij} and corresponding rotor,

$$\exp\left(\frac{\Delta}{2} \mathbf{e}_{ij}\right). \tag{2.5}$$

Consider the Taylor expansion of this expression in a geometric algebra without yet identifying the signature of the algebra:

$$\exp\left(\frac{\Delta}{2} \mathbf{e}_{ij}\right) = 1 + \frac{\Delta}{2} \mathbf{e}_{ij} + \frac{(\Delta/2)^2}{2!} \mathbf{e}_{ij}^2 + \frac{(\Delta/2)^3}{3!} \mathbf{e}_{ij}^3 + \frac{(\Delta/2)^4}{4!} \mathbf{e}_{ij}^4 + \dots \tag{2.6}$$

$Q(\mathbf{e}_i)$	$Q(\mathbf{e}_j)$	\mathbf{e}_{ij}^2
1	-1	1
-1	1	1
1	1	-1
-1	-1	-1
Either is 0		0

Table 2.2: Value of \mathbf{e}_{ij}^2 for various signatures.

If a vector v is perpendicular to both \mathbf{e}_i and \mathbf{e}_j , then $\mathbf{e}_{ji}v = v\mathbf{e}_{ji}$. It follows that v commutes with every term in the Taylor series expansion in Equation 2.6 and commutes with the entire expression. Hence,

$$\exp\left(\frac{\Delta}{2}\mathbf{e}_{ij}\right)v\exp\left(-\frac{\Delta}{2}\mathbf{e}_{ij}\right) = v\exp\left(\frac{\Delta}{2}\mathbf{e}_{ij}\right)\exp\left(-\frac{\Delta}{2}\mathbf{e}_{ij}\right) = v.$$

In essence, when the element v is perpendicular to \mathbf{e}_i and \mathbf{e}_j , the application of the rotor in Equation 2.5 results in no change to the vector. Therefore, it suffices to consider the effects of this rotor on the elements \mathbf{e}_i and \mathbf{e}_j .

We now identify the effects of the choice of signature. We note that

$$\mathbf{e}_{ij}^2 = \mathbf{e}_i\mathbf{e}_j\mathbf{e}_i\mathbf{e}_j = -\mathbf{e}_i\mathbf{e}_j\mathbf{e}_j\mathbf{e}_i = -Q(\mathbf{e}_i)Q(\mathbf{e}_j)$$

and thus the effects of the possible signatures are listed in Table 2.2.

We now observe in detail what each possible value of \mathbf{e}_{ij}^2 implies for the Taylor series of Equation 2.6 and the resulting transformation. We then describe how transformations are composed together given a fixed signature.

When $\mathbf{e}_{ij}^2 = -1$ — Rotation

When $\mathbf{e}_{ij}^2 = -1$ we observe the Taylor series to be

$$\begin{aligned} \exp\left(\frac{\Delta}{2}\mathbf{e}_{ij}\right) &= 1 + \frac{\Delta}{2}\mathbf{e}_{ij} - \frac{(\Delta/2)^2}{2!} - \frac{(\Delta/2)^3}{3!}\mathbf{e}_{ij} + \frac{(\Delta/2)^4}{4!} + \dots \\ &= \cos(\Delta/2) + \sin(\Delta/2)\mathbf{e}_{ij} \end{aligned}$$

and thus we have

$$\begin{aligned} \exp\left(\frac{\Delta}{2}\mathbf{e}_{ij}\right)v\exp\left(-\frac{\Delta}{2}\mathbf{e}_{ij}\right) &= (\cos(\Delta/2) + \sin(\Delta/2)\mathbf{e}_{ij})v(\cos(\Delta/2) - \sin(\Delta/2)\mathbf{e}_{ij}) \\ &= \cos^2(\Delta/2)v - \sin^2(\Delta/2)\mathbf{e}_{ij}v\mathbf{e}_{ij} \\ &\quad + \sin(\Delta/2)\cos(\Delta/2)\mathbf{e}_{ij}v - \sin(\Delta/2)\cos(\Delta/2)v\mathbf{e}_{ij}. \end{aligned}$$

If $v = \mathbf{e}_i$, then we have

$$\mathbf{e}_{ij} v \mathbf{e}_{ij} = Q(\mathbf{e}_i)Q(\mathbf{e}_j)\mathbf{e}_i = \mathbf{e}_i$$

and

$$v \mathbf{e}_{ij} = \mathbf{e}_j = \mathbf{e}_{ji} v = -\mathbf{e}_{ij} v$$

and hence

$$\begin{aligned} \exp\left(\frac{\Delta}{2}\mathbf{e}_{ij}\right) \mathbf{e}_i \exp\left(-\frac{\Delta}{2}\mathbf{e}_{ij}\right) &= \left(\cos^2(\Delta/2) - \sin^2(\Delta/2)\right)\mathbf{e}_i + \left(2\cos(\Delta/2)\sin(\Delta/2)\right)\mathbf{e}_j \\ &= \cos(\Delta)\mathbf{e}_i + \sin(\Delta)\mathbf{e}_j. \end{aligned}$$

We can use similar logic to show that

$$\exp\left(\frac{\Delta}{2}\mathbf{e}_{ij}\right) \mathbf{e}_j \exp\left(-\frac{\Delta}{2}\mathbf{e}_{ij}\right) = \cos(\Delta)\mathbf{e}_j - \sin(\Delta)\mathbf{e}_i$$

and hence we see that the rotor $\exp(\Delta/2 \mathbf{e}_{ij})$ represents the rotation from \mathbf{e}_i to \mathbf{e}_j .

When $\mathbf{e}_{ij}^2 = 0$ — Shear

When $\mathbf{e}_{ij}^2 = 0$, the Taylor series simplifies to

$$\exp\left(\frac{\Delta}{2}\mathbf{e}_{ij}\right) = 1 + \frac{\Delta}{2}\mathbf{e}_{ij}.$$

Then applying this rotor as a versor we get

$$\begin{aligned} \exp\left(\frac{\Delta}{2}\mathbf{e}_{ij}\right) v \exp\left(-\frac{\Delta}{2}\mathbf{e}_{ij}\right) &= \left(1 + \frac{\Delta}{2}\mathbf{e}_{ij}\right)v\left(1 - \frac{\Delta}{2}\mathbf{e}_{ij}\right) \\ &= v + \frac{\Delta}{2}\mathbf{e}_{ij} v - \frac{\Delta}{2}v \mathbf{e}_{ij} + \frac{\Delta}{2}\mathbf{e}_{ij} v \frac{\Delta}{2}\mathbf{e}_{ij}. \end{aligned}$$

Since one of \mathbf{e}_i^2 or \mathbf{e}_j^2 is 0, we see that the fourth term must be 0. If we have $\mathbf{e}_i^2 = \mathbf{e}_j^2 = 0$ then the second and third terms are also equal to 0, and we see that the rotor does not affect any vectors at all. If $\mathbf{e}_j^2 \neq 0$ then we have

$$\begin{aligned} \exp\left(\frac{\Delta}{2}\mathbf{e}_{ij}\right) \mathbf{e}_j \exp\left(-\frac{\Delta}{2}\mathbf{e}_{ij}\right) &= \mathbf{e}_j + \frac{\Delta}{2}Q(\mathbf{e}_j)\mathbf{e}_i + \frac{\Delta}{2}Q(\mathbf{e}_j)\mathbf{e}_i \\ &= \mathbf{e}_j + \Delta Q(\mathbf{e}_j)\mathbf{e}_i \end{aligned}$$

and, since $\mathbf{e}_i^2 = 0$, it can be shown

$$\exp\left(\frac{\Delta}{2}\mathbf{e}_{ij}\right) \mathbf{e}_i \exp\left(-\frac{\Delta}{2}\mathbf{e}_{ij}\right) = \mathbf{e}_i,$$

i.e., applying the rotor as a versor does not modify the vector \mathbf{e}_i . Therefore, the rotor performs the transformation

$$\mathbf{e}_j \rightarrow \mathbf{e}_j + Q(\mathbf{e}_j)\mathbf{e}_i$$

while not transforming any other basis vectors. Thus, the rotor performs a shear in the direction of \mathbf{e}_i measured by $Q(\mathbf{e}_j)[\mathbf{e}_j]$.

When $e_{ij}^2 = 1$ — Hyperbolic Rotation

In this case, the rotor's Taylor series is

$$\exp\left(\frac{\Delta}{2}\mathbf{e}_{ij}\right) = \cosh(\Delta/2) + \sinh(\Delta/2)\mathbf{e}_{ij}$$

and the rotor corresponds to hyperbolic rotations.

To create rigid-body transformations in a homogeneous coordinate system, we will use rotations and shear transformations. However, hyperbolic rotations are not relevant to rigid-body transformations, and so we do not go into detail here.

2.4.2 Composing Transformations Together

It is sometimes desirable to compose two transformations together into one transformation. Consider the case where we have 2-blades A and B where A and B are orthogonal. Then the transformations $\exp(A)$ and $\exp(B)$ affect different subspaces of the total vector space. Thus, each transformation can be done independently without affecting one another. Hence $\exp(A)\exp(B) = \exp(B)\exp(A)$. Algebraically, since A and B are orthogonal 2-blades, $AB = BA$ and thus

$$\exp(A)\exp(B) = \exp(A+B) = \exp(B)\exp(A).$$

However, we want to consider the case where A and B are not necessarily orthogonal. In that case, it is not necessarily true that $AB = BA$ or that $\exp(A)\exp(B) = \exp(A+B)$. However, we can use the Lie product formula [12]:

$$\lim_{k \rightarrow \infty} (e^{\frac{1}{k}A}e^{\frac{1}{k}B})^k = e^{A+B}.$$

In particular, the formula $(e^{\frac{1}{k}A}e^{\frac{1}{k}B})^k$ corresponds to repeatedly applying $1/k$ th of the rotor A and then $1/k$ th of the rotor B k times. In the limit, this is equivalent to applying both motions simultaneously. This enables us to use the analysis of Section 2.4.1 of each basis blade to analyze the effects of bivectors in general.

Consider the rotor

$$\exp\left(\frac{\Delta}{2}(\mathbf{e}_2 + \mathbf{e}_3) \wedge \mathbf{e}_1\right) = \exp\left(\frac{\Delta}{2}(\mathbf{e}_{21} + \mathbf{e}_{31})\right). \quad (2.7)$$

The elements \mathbf{e}_{21} and \mathbf{e}_{31} are not orthogonal. However, we can view the transformation as applying

$$\exp\left(\frac{\Delta}{2}\mathbf{e}_{21}\right) \quad \text{and} \quad \exp\left(\frac{\Delta}{2}\mathbf{e}_{31}\right)$$

simultaneously. For example, if $Q(\mathbf{e}_1) = 1$ and $Q(\mathbf{e}_2) = Q(\mathbf{e}_3) = 0$, then \mathbf{e}_{21} and \mathbf{e}_{31} correspond to shear transformations. The transformation \mathbf{e}_{21} corresponds to shearing in the direction \mathbf{e}_2 measured by $1[\mathbf{e}_1]$ and the transformation \mathbf{e}_{31} corresponds to shearing in the direction \mathbf{e}_3 measured by $1[\mathbf{e}_1]$. It follows that the transformation in Equation 2.7 corresponds to the transformation of shearing in direction $\mathbf{e}_2 + \mathbf{e}_3$ measured by $\sqrt{2}[\mathbf{e}_1]$.

2.5 Projective Geometric Algebra

Projective Geometric Algebra (also called *Plane-based Geometric Algebra*) (PGA) is the application of homogeneous coordinates to geometric algebra [6, 16]. Instead of representing rigid-body motions by matrices, we instead represent these transformations by versors (and in particular, rotors). As our running example, we will specifically construct the PGA for 3D Euclidean space. Just as in the homogeneous coordinates system, we begin with \mathbf{e}_1 , \mathbf{e}_2 and \mathbf{e}_3 as our Euclidean axes and extend our space by including a fourth projective axis, \mathbf{e}_0 . We will place all finite points on the affine hyperplane. The notation used in this section is a non-standard combination of Dorst's notation [6] and Lengyel and De Keninck's notation [16]. See Appendix D for a comparison of the notation of this thesis, that of Dorst and De Keninck and that of Lengyel.

We now need to determine the signature of the algebra. For Euclidean vectors \mathbf{e}_i and \mathbf{e}_j , we desire \mathbf{e}_{ij} to correspond to rotations and for \mathbf{e}_{0i} to correspond to a shear transformation. For \mathbf{e}_{ij} to represent a rotation, we need either $Q(\mathbf{e}_i) = Q(\mathbf{e}_j) = 1$ or $Q(\mathbf{e}_i) = Q(\mathbf{e}_j) = -1$ (Table 2.2). Since this must be true for any pair of Euclidean axes \mathbf{e}_i and \mathbf{e}_j , we see that the signature must be consistent for all Euclidean axes. In essence, we require either

- $Q(\mathbf{e}_i) = 1$ for all Euclidean axes \mathbf{e}_i , or
- $Q(\mathbf{e}_i) = -1$ for all Euclidean axes \mathbf{e}_i .

Without loss of generality, let $Q(\mathbf{e}_i) = 1$ for all Euclidean axes \mathbf{e}_i . The final choice of signature is that of \mathbf{e}_0 . To enable a shear transformation for the purpose of creating a translation transformation in the affine hyperplane, we require that $\mathbf{e}_{0i}^2 = 0$. Since $Q(\mathbf{e}_i) = 1$, it follows that $Q(\mathbf{e}_0) = 0$. The signature of the algebra is therefore:

$$Q(\mathbf{e}_0) = 0 \quad \text{and} \quad Q(\mathbf{e}_i) = 1 \text{ for all Euclidean } \mathbf{e}_i.$$

Unlike in the homogeneous coordinate system, we will have two ways of representing points: the direct representation and the dual representation. The direct representation is identical to the homogeneous system, that is the finite point (v_1, \dots, v_n) is represented by the vector

$$p = \vec{v} + \mathbf{e}_0 = \vec{v}_1 \mathbf{e}_1 + \vec{v}_2 \mathbf{e}_2 + \dots + \vec{v}_n \mathbf{e}_n + \mathbf{e}_0.$$

The dual representation of the finite point is its left complement

$$\underline{p} = \underline{\vec{v}} + \underline{\mathbf{e}_0} = \vec{v}_1 \underline{\mathbf{e}_1} + \vec{v}_2 \underline{\mathbf{e}_2} + \dots + \vec{v}_n \underline{\mathbf{e}_n} + \underline{\mathbf{e}_0}.$$

Similarly, a point at infinity represented by \vec{v} can be dually represented by the pseudovector $\underline{\vec{v}}$. When performing rigid-body transformations via versors, we must apply the versor to the dual representation of the point. Thus, the application of a versor to a point (v_1, \dots, v_n) will be performed as

$$V \underline{\vec{v}} + \underline{\mathbf{e}_0} V^{-1}.$$

The justification for using the dual representation is detailed in the following section.

It is worth noting that in an n -dimensional PGA, the pseudoscalar is

$$\mathbb{1} = \mathbf{e}_{12\dots n0},$$

that is, we place the projective axis as the right-most axis in the pseudoscalar. This matches the convention of Lengyel [16] but is the opposite convention of Dorst and De Keninck [6] as discussed in Appendix D.

2.5.1 Dual Representation Justification

We now justify applying the transformations to the dual representation of points in PGA to achieve rigid-body transformations as rotors. Recall from Subsection 2.4.1 that a rotor of the form $\mathbf{e}_{ij}^2 = 0$ performs shear. In particular, notice that to mimic translation in the affine hyperplane, we want the rotor associated with \mathbf{e}_{0i} to perform shear in the direction of $\pm \mathbf{e}_i$ measured by $1[\mathbf{e}_0]$ (the sign of the direction can be adjusted after the fact). However, when applying this rotor to the direct representation of points, the transformation is the wrong shear transformation:

$$\begin{aligned} \exp\left(\frac{\Delta}{2}\mathbf{e}_{0i}\right) \mathbf{e}_i \exp\left(-\frac{\Delta}{2}\mathbf{e}_{0i}\right) &= \mathbf{e}_i + \Delta Q(\mathbf{e}_i)\mathbf{e}_0, \text{ and} \\ \exp\left(\frac{\Delta}{2}\mathbf{e}_{0i}\right) \mathbf{e}_0 \exp\left(-\frac{\Delta}{2}\mathbf{e}_{0i}\right) &= \mathbf{e}_0. \end{aligned}$$



Figure 2.5: A depiction of the shear transformation being applied to direct representation of points in PGA featuring a Euclidean axis (\mathbf{e}_1) and a projective axis (\mathbf{e}_0). Red dots mark the points in the scene. A dotted line denotes the affine hyperplane. (a) The scene before the shear transformation and (b) the scene after the shear transformation. The axis-aligned blue lines are tilted in (b) to show the effects of shear.

In particular, the rotor $\exp(\Delta/2 \mathbf{e}_{i0})$ performs a shear in the direction \mathbf{e}_0 measured by $1[\mathbf{e}_i]$. See Figure 2.5 for an illustration. Thus, the rotor performs the transpose of the desired transformation.

As discussed in Subsection 2.3.4, for compositions of shear and rotation transformations, when the transformation M is applied to vectors, the inverse transpose transformation M^{-T} is applied to the pseudovectors. Since rotations are orthogonal transformations, for any rotation matrix M_r we have $M_r^{-T} = M_r$, i.e., rotations are applied to pseudovectors identically to vectors. However, for the shear transformation, the transformation on pseudovectors is quite different:

$$\begin{aligned}
\exp\left(\frac{\Delta}{2} \mathbf{e}_{0i}\right) \underline{\mathbf{e}}_0 \exp\left(-\frac{\Delta}{2} \mathbf{e}_{0i}\right) &= \exp\left(\frac{\Delta}{2} \mathbf{e}_{0i}\right) \mathbf{e}_{12\dots n} \exp\left(-\frac{\Delta}{2} \mathbf{e}_{0i}\right) \\
&= (\mathbf{e}_{12\dots(i-1)}) \exp\left(\frac{\Delta}{2} \mathbf{e}_{0i}\right) \mathbf{e}_i \exp\left(-\frac{\Delta}{2} \mathbf{e}_{0i}\right) (\mathbf{e}_{(i+1)\dots n}) \\
&= (\mathbf{e}_{12\dots(i-1)}) (\mathbf{e}_i + \Delta Q(\mathbf{e}_i) \mathbf{e}_0) (\mathbf{e}_{(i+1)\dots n}) \\
&= \mathbf{e}_{12\dots n} + \Delta Q(\mathbf{e}_i) \mathbf{e}_{12\dots(i-1)0(i+1)\dots n} \\
&= \underline{\mathbf{e}}_0 - \Delta Q(\mathbf{e}_i) \underline{\mathbf{e}}_i \\
&= \underline{\mathbf{e}}_0 - \Delta Q(\mathbf{e}_i) \mathbf{e}_i
\end{aligned}$$

and

$$\begin{aligned}
\exp\left(\frac{\Delta}{2}\mathbf{e}_{0i}\right)\underline{\mathbf{e}}_i\exp\left(-\frac{\Delta}{2}\mathbf{e}_{0i}\right) &= \exp\left(\frac{\Delta}{2}\mathbf{e}_{0i}\right)(-\mathbf{e}_{12\dots(i-1)0(i+1)\dots n})\exp\left(-\frac{\Delta}{2}\mathbf{e}_{0i}\right) \\
&= -(\mathbf{e}_{12\dots(i-1)})\exp\left(\frac{\Delta}{2}\mathbf{e}_{0i}\right)\mathbf{e}_0\exp\left(-\frac{\Delta}{2}\mathbf{e}_{0i}\right)(\mathbf{e}_{(i+1)\dots n}) \\
&= -\mathbf{e}_{12\dots(i-1)}\mathbf{e}_0\mathbf{e}_{(i+1)\dots n} \\
&= \underline{\mathbf{e}}_i
\end{aligned}$$

and thus we have the shear transformation

$$\mathbf{e}_0 \rightarrow \mathbf{e}_0 - \Delta Q(\mathbf{e}_i)\mathbf{e}_i$$

applied within the dual space. In summary,

$$\begin{array}{c}
\mathbf{Vectors} \\
\text{a shear in direction } \mathbf{e}_0 \text{ measured by } 1[\mathbf{e}_i] \\
\updownarrow \\
\text{a shear in direction } -\mathbf{e}_i \text{ measured by } 1[\mathbf{e}_0] \\
\mathbf{Pseudovectors}
\end{array}$$

So we can use the blade $\mathbf{e}_{i0} = -\mathbf{e}_{0i}$ to perform shear transformations in the direction \mathbf{e}_i measured by $1[\mathbf{e}_0]$. Thus, we have:

- the transformation associated with \mathbf{e}_{ij} performs a rotation on the dual representation of a point, and
- the transformation associated with \mathbf{e}_{i0} performs the shear transformation that causes translation on the dual representation of a point.

Hence, we use the dual representation of points when applying transformations on points in PGA.

2.5.2 Lines and Planes

In the homogeneous coordinate system, vectors that intersected the affine hyperplane at position $\vec{v} + \mathbf{e}_0$ represented the point (v_1, \dots, v_n) . In PGA, the direct representation of points is identical. However, the exterior algebra allows us to create elements that represent linear subspaces. These new elements allow us to create elements that represent lines and planes that are offset from the origin in PGA. See Figure 2.6 for an illustration of a line offset from the origin.

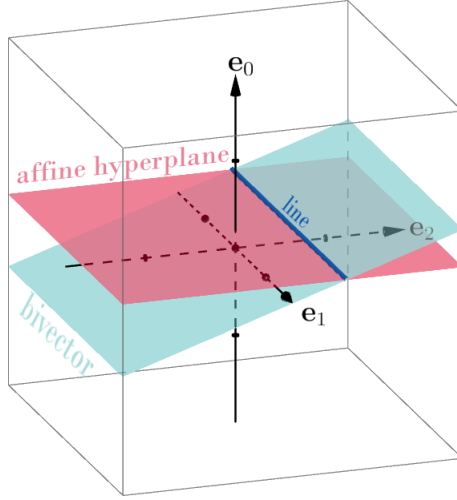


Figure 2.6: A depiction of an offset line in PGA. The red plane is the affine hyperplane. The blue plane is a bivector. The dark blue line is the line at which they intersect. The line is offset from the origin.

For example, consider the finite points $p_1 = \vec{v} + \mathbf{e}_0$ and $p_2 = \vec{w} + \mathbf{e}_0$. The exterior product of these elements $p_1 \wedge p_2$ corresponds to a 2D linear subspace. The set of finite points that lie in the linear subspace of $p_1 \wedge p_2$ must have a coefficient of 1 for the \mathbf{e}_0 axis. Thus, every point in the linear subspace of $p_1 \wedge p_2$ must be of the form

$$\alpha p_1 + (1 - \alpha)p_2$$

for some scalar $\alpha \in \mathbb{R}$. In essence, the element $p_1 \wedge p_2$ is a direct representation of the line $l(\alpha) = \alpha p_1 + (1 - \alpha)p_2$ because

$$(p_1 \wedge p_2) \wedge p = 0 \iff p = \alpha p_1 + (1 - \alpha)p_2.$$

Additionally, one can show that points at infinity behave in a geometrically intuitive way with the construction of finite lines: the exterior product of a finite point p_1 and a point at infinity \vec{v} creates a finite line that contains p_1 and points in the direction \vec{v} .

Just as the homogeneous coordinate systems contain points at infinity, PGA contains *lines at infinity*. In particular, the exterior product of two points at infinity creates a line at infinity. For example, the exterior product of points at infinity \vec{v} and \vec{w} creates the element $\vec{v} \wedge \vec{w}$ where

$$(\vec{v} \wedge \vec{w}) \wedge u = 0 \iff u = \alpha \vec{v} + \beta \vec{w}.$$

Blade	Direct Representation	Dual Representation
0-blade (scalar)	—	—
1-blade (vector)	Point	Plane
2-blade	Line	Line
3-blade (pseudovector)	Plane	Point
4-blade (pseudoscalar)	—	—

Table 2.3: A table of blades and their corresponding direct and dual representations for 3D PGA.

In essence, u must be purely Euclidean and thus represents a point at infinity. Hence, the line itself is at infinity. We call the set of finite lines and lines at infinity as simply *lines*.

Similar to 2-blades representing lines, one can show that the exterior product of three finite points corresponds to a finite plane. Additionally, the exterior product of three infinite points represents a *plane at infinity*.

2.5.3 Duals of Lines and Planes

Just as there are dual representations of points, there are also dual representations of lines and planes. In particular, given a 2-blade ℓ that represents a line and 3-blade P that represents a plane, the elements that dually represent the line and plane are $\underline{\ell}$ and \underline{P} respectively. In 3D PGA, the dual representation of a plane, \underline{P} , is a 1-blade (i.e., a vector). Thus, we see that vectors can both directly represent points and dually represent planes. Similarly, 3-blades directly represent planes and dually represent points. A 2-blade both directly and dually represents a line, but these lines are distinct. There is no geometric interpretation of scalars and pseudoscalars. These results are summarized in Table 2.3.

In essence, the algebra has two distinct methods of representing points, lines and planes. Dorst and De Keninck [6] consider the dual representation as the default, considering vectors to represent planes and performing intersections of these planes to form lines and points via the exterior product. In this thesis, we present the direct representation as being the default to match the convention of homogeneous coordinates. Lengyel [16] similarly uses the direct representation as the default, but introduces a new product, called the *geometric antiproduct*, such that versors can be applied to direct representation of elements rather than their dual representation. In both Dorst and De Keninck’s model and Lengyel’s model, rotations around a line can be performed by exponentiating the line [6, 16]. In the model presented in this paper, we can perform a rotation around a line ℓ by exponentiating its complement. That is, the rotor

$$\exp(\underline{\ell})$$

performs a rotation around the line ℓ . If $(\underline{\ell})^2 = -1$, then the coefficient corresponds to half

the angle of rotation, that is,

$$\exp\left(\frac{\theta}{2}\underline{\ell}\right)$$

performs a rotation of θ around the line ℓ .

2.5.4 Euclidean Dual and Cross Product

In PGA, the complement of a Euclidean vector results in an element that contains a factor of \mathbf{e}_0 , i.e., the element is not Euclidean. It is sometimes useful to consider the dual of an element purely in the Euclidean space. For example, in 3D PGA, given a plane represented by \mathbf{e}_{23} , one would hope to get the vector \mathbf{e}_1 rather than \mathbf{e}_{10} . We define the Euclidean dual of a Euclidean element E as

$$\underline{E}\mathbf{e}_0.$$

In 3D PGA, the Euclidean dual of a 2-blade corresponds to the cross product of the blade's components. That is to say, given Euclidean vectors a and b , the cross product is

$$a \times b = \underline{(a \wedge b)}\mathbf{e}_0.$$

2.6 The Translation Frame, The Bishop Frame and Frenet-Serret Frame

A *coordinate frame* (from now on, simply referred to as a *frame*) is a basis for the vector space associated with a point of origin. Since Euclidean motions maintain distances between points, it is necessary and sufficient to be able to describe the outcome of a Euclidean motion by a change from one orthogonal frame to another (without changing the handedness of the basis).

Given a continuous differentiable parametric curve in 3D space, it is often desirable to associate that curve with a moving frame. There are many possible frames one can associate with a curve [2]. In this section, we suppose the parametric curve is the differentiable function

$$f_{\bullet}(t) = f_1(t)\mathbf{e}_1 + f_2(t)\mathbf{e}_2 + f_3(t)\mathbf{e}_3.$$

We assume our starting frame has $f_{\bullet}(0)$ as our point of origin. For each frame, we always assume the frame's origin is $f_{\bullet}(t)$ for each time t . The frame's initial set of basis vectors will depend on how we want to associate the frame's basis with the curve, and thus differs in each section.

2.6.1 The Translation Frame

A simple moving frame we can associate with this curve is letting the frame's origin be $f_{\bullet}(t)$ while not changing the basis of the frame. We will refer to this frame as the *translation frame* of the parametric curve. In essence, the frame translates but never rotates.

The frame's basis vectors do not have any significance to the moving frame, so we can arbitrarily pick the frame's starting basis to be any basis. In this thesis, we will pick the frame's starting basis to match that of the Frenet-Serret frame when possible to allow for an easy visual comparison. However, this is not a suitable strategy in general since the Frenet-Serret frame has stricter requirements for the parametric curve $f_{\bullet}(t)$. A simple basis for the frame that will always work is $(\mathbf{e}_1, \mathbf{e}_2, \mathbf{e}_3)$.

2.6.2 The Bishop Frame

If the curve is twice differentiable with f' always being non-zero, another reasonable choice for associating a parametric curve with a moving frame is to match the frame's orientation with the tangent vector of the curve [2]. Hence, we set one of the frame's basis vectors to match the tangent vector at time 0 and subsequently perform rotations to ensure this basis vector always matches the curve's tangent. We refer to this basis vector as the frame's *forward direction*. The plane of rotation moving the frame's forward direction is called the *osculating plane* [20]. The local curvature of the parametric curve has an associated circle that "kisses" the line and has the same curvature. This circle is referred to as the *osculating circle*. See Figure 2.7 for an illustration. The direction pointing towards the circle's center is called the *normal* of the curve. Note that the osculating plane, osculating circle and normal only exist if the local curvature of the parametric curve is non-zero.

Fixing the frame's forward direction to point in the direction of the tangent vector leaves one degree of freedom in 3D (and more degrees of freedom in higher dimensions). In 3D, the extra degree of freedom allows for rotation in the plane perpendicular to the tangent vector. This plane is referred to as the *normal plane* [20]. The extra degree of freedom that corresponds to rotation in the normal plane is called *torsion*.

A natural choice is to set the torsion to 0. If we do so, we get the *Bishop frame* [2], also called the *Parallel Transport Frame* [11] or *Rotation-Minimizing Frame* [26]. This frame is well-defined even when the curvature of the curve is zero. However, note that although the forward direction of the frame is the tangent vector of the curve, the left and down directions of the frame cannot be determined by local features of the curve. Instead, the left and down directions depend on the choice of starting frame and accumulation of rotation effects from the starting time to the time of interest.

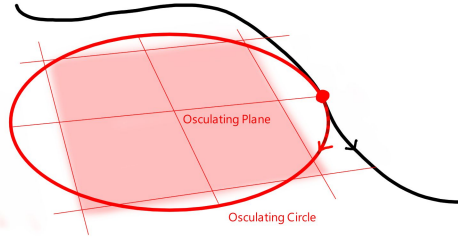


Figure 2.7: A depiction of the osculating circle. The black line is the parametric curve. The red dot is the point f . The red circle is the osculating circle. The faint red grid is the osculating plane.

2.6.3 The Frenet-Serret Frame and Darboux Vector

If we assume the progression and the curvature of our curve is non-zero, i.e., the values of f' and f'' are always non-zero, then the osculating plane always exists. If the curve f is also thrice differentiable, then the osculating plane transforms smoothly, rotating about the tangent vector. The *Frenet-Serret frame* [21] is formed by adding torsion to the transformation to match the rotation of the osculating plane. Another perspective is that while maintaining the frame's forward direction to be the curve's tangent vector, we maintain a perpendicular basis vector to be the curve's normal. We refer to the basis vector matching the curve's normal as the *downward direction*. See Figure 2.8 for an illustration.

To find the Frenet-Serret frame of a curve, we first define the tangent vector to be $\mathbf{T} = f'_{\bullet} / \|f'_{\bullet}\|$. The value of \mathbf{T} is well-defined since $\|f'_{\bullet}\| \neq 0$. The value of \mathbf{T}' points in the direction of the normal vector, and since we assume f'' is non-zero, $\mathbf{T}' = f''_{\bullet} / \|f'_{\bullet}\|$ is also non-zero. Hence, we define the normal vector to be $\mathbf{N} = \mathbf{T}' / \|\mathbf{T}'\|$. The unit vector perpendicular to both \mathbf{T} and \mathbf{N} that is required to form a basis in 3D is referred to as the *binormal*, and is denoted $\mathbf{B} := \mathbf{T} \times \mathbf{N}$. The point of origin $f_{\bullet}(t)$ and the basis vectors $\mathbf{T}(t)$, $\mathbf{N}(t)$ and $\mathbf{B}(t)$ constitute our frame at time t . The curvature of the frame is defined by $\kappa := \|f''_{\bullet}\|$ [21] and its reciprocal $1/\kappa$ is the radius of the osculating circle. The torsion [21] is

$$\tau := -\mathbf{N} \cdot \mathbf{B}'.$$

A summary of these results is given in Table 2.4.

Since the frame at any point f_{\bullet} is fully determined by f_{\bullet} (the origin), f'_{\bullet} (the forward direction) and f''_{\bullet} (the downward direction), then unlike the Bishop frame, the Frenet-Serret frame is fully determined by local features of the curve. However, recall that this frame is only defined for points on the curve that have non-zero curvature.

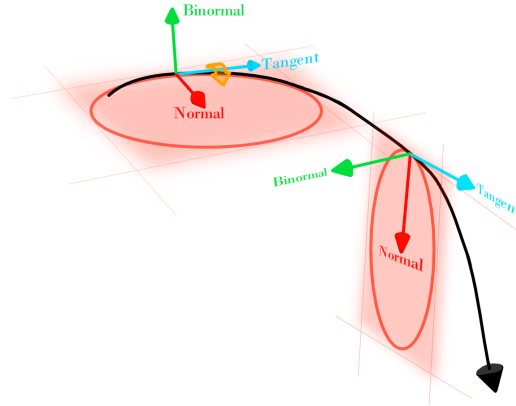


Figure 2.8: A depiction of the moving osculating plane in the Frenet-Serret frame. The black line is the parametric curve. The Frenet-Serret frame, the osculating circle with a faint grid representing the osculating plane is depicted at two moments in time. At the first moment in time, an orange arrow around the tangent vector indicates the torsion rotation.

Component	Symbol	Value
Origin	O	f_{\bullet}
Tangent	\mathbf{T}	$f'_{\bullet}/\ f'_{\bullet}\ $
Normal	\mathbf{N}	$\mathbf{T}'/\ \mathbf{T}'\ $
Binormal	\mathbf{B}	$\mathbf{T} \times \mathbf{N}$
Curvature	κ	$\ \mathbf{T}'\ $
Torsion	τ	$-\mathbf{N} \cdot \mathbf{B}'$

Table 2.4: A table of functions for the Frenet-Serret frame for the function f_{\bullet} .

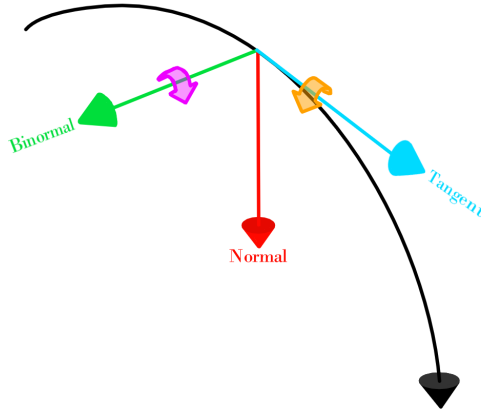


Figure 2.9: A depiction of the components of a Darboux vector. The black line is the parameterized curve. The purple arrow around the binormal vector indicates the rotation within the osculating plane, i.e., the purple arrow represents $\kappa\mathbf{B}$. The orange arrow around the tangent vector indicates the torsion rotation, i.e., the orange arrow represents $\tau\mathbf{T}$.

The angular velocity of the point on the curve can be represented by the *Darboux vector* [26]

$$\omega = \tau\mathbf{T} + \kappa\mathbf{B}.$$

Using the right-hand rule, we have that the point $f(t)$ rotates in the plane perpendicular to $\mathbf{B}(t)$ (that is, the osculating plane) by amount $\kappa(t)$ and in the plane perpendicular to $\mathbf{T}(t)$ (that is, the normal plane) by amount $\tau(t)$. See Figure 2.9 for an illustration of the components of the Darboux vector. This angular velocity vector describes the rotation of the point as though it were a fixed point in space. In essence, the Darboux vector represents the rotation of the basis of the frame, but not the change in the frame's origin. Although the linear algebra construction normally constructs the Darboux element as a vector, since the element represents a combination of rotations, it is more accurate in geometric algebra to construct it as a bivector. Hence, we prefer to view the Darboux vector as the left complement

$$\underline{\omega} = \tau\underline{\mathbf{T}} + \kappa\underline{\mathbf{B}}.$$

2.7 Related Work

PGA is a relatively new subfield of geometric algebra. PGA was first introduced by Gunn [10] in 2019. Since then, Dorst and De Keninck [6] and Lengyel [16] have made

contributions developing PGA. Since PGA is such a new framework, resources for computing in PGA are limited. To perform computations and to create visualizations for PGA, my supervisor and I created a MATLAB package called PGABLE [15]. Unlike this thesis, which uses a combination of conventions and notation from both Dorst and De Keninck and Lengyel, the software package PGABLE follows the conventions of Dorst and De Keninck. Another MATLAB package that is able to perform PGA computations is SUGAR [24]. Velasco et al. have written about using PGA in SUGAR to compute the motion of kinematic chains [25]. These kinematic chains are somewhat similar to moving frames in the sense that they involve the successive application of rotors. However, these rotors are constructed for discrete points (at the joints of a robotic arm) and the angles of rotation are chosen by the user. Unlike PGABLE, SUGAR does not have built-in visualizations for PGA.

The Frenet-Serret frame and other frames fitted to curves are well understood [2, 20, 21]. A significant contribution to the field of associating frames to parametric curves was written by Bishop [2] in which the author defines the Bishop frame. The author describes how the development of frames can be described via differential equations. In particular, given

$$\mathbf{F} = \begin{bmatrix} \mathbf{F}_1 \\ \mathbf{F}_2 \\ \vdots \\ \mathbf{F}_n \end{bmatrix}$$

where $\mathbf{F}_1, \dots, \mathbf{F}_n$ forms an orthogonal basis for the frame, then the local motion of frames can be written in the form

$$\mathbf{F}' = M\mathbf{F} \tag{2.8}$$

for some skew-symmetric matrix M . The Frenet-Serret frame can be described via a differential equation of the form

$$\mathbf{F}' = \begin{bmatrix} 0 & \kappa & 0 \\ -\kappa & 0 & \tau \\ 0 & -\tau & 0 \end{bmatrix} \mathbf{F}$$

and the development of the Bishop frame can be described via

$$\mathbf{F}' = \begin{bmatrix} 0 & k_1 & k_2 \\ -k_1 & 0 & 0 \\ -k_2 & 0 & 0 \end{bmatrix} \mathbf{F} \tag{2.9}$$

for particular values of κ, τ, k_1 and k_2 . Thus, the transformation of the basis vectors of a frame at a particular position on the curve can be fully described by these differential equations. The terms κ, τ, k_1 and k_2 can be computed via the parametric curve $f_{\bullet}(s)$.

One application of moving frames is to create a polygonal tube around a parametric curve f . We can do so by repeatedly applying the curve's moving frame transformation

to a polygon fitted around the point $f(0)$. Assuming our time step is $\Delta \in \mathbb{R}$, we start with the starting frame basis \mathbf{F}^1 and successively create $\mathbf{F}^i \rightarrow \mathbf{F}^{i+1}$ by approximating the following time step's frame basis using Equation 2.8. At each iteration, we perform a rotation and a translation on the set of points forming the corners of the polygon. The rotation corresponds to the rotation from \mathbf{F}^i to \mathbf{F}^{i+1} , and the translation corresponds to the translation from $f(\Delta i)$ to $f(\Delta(i+1))$.

Since these computations involve successive applications of 3D rotations, it is natural to want to apply these rotations via quaternions. Hanson shows how to use quaternions to describe the rotations of the Frenet-Serret frame [13]. Unlike the results of this thesis, Hanson's results do not cover the case of higher-dimensional extensions of the Frenet-Serret frame. If one is interested in the Bishop frame for the 3D case, Wang et al. describes a more sophisticated method of performing the transformation of Equation 2.9 for Bishop frames to reduce computational error [26]. Kneza et al. used the methods of Wang et al. in combination with geometric algebra to perform rotation minimizing (Bishop frame) transformations in the Minkowski space $\mathbb{R}^{2,1}$ [19].

To tackle higher-dimensional extensions of the Bishop frame, Gökçelik et al. describe the Bishop frame in the 4-dimensional case using linear algebra methods [11]. Similarly, Ross uses linear algebra to define higher-dimensional generalizations of the Frenet-Serret frame [23]. Unlike the work of this thesis, these results do not employ geometric algebra, nor do they include the translation of the frame's origin in their description of the rigid-body motion of the moving frame.

Moving frames can also be used to simulate deformable bodies. Similarly to creating a tube that is fitted around a curve, one can use moving frames to simulate an elastic rod. Bergou et al. define a *material frame* for an elastic rod by representing it as the angular deviation from the Bishop frame [1]. Lipman et al. use moving frames to perform volume-preserving deformation of meshes [18].

This thesis is limited in that it only covers frames associated with parametric curves. Moving frames can also be constructed for general surfaces. The application of moving frames with surface theory has been covered by Darling [5] where the author discusses constructing orthonormal frames from surfaces with multiple parameters.

Chapter 3

Local Motion Rotors

We wish to create elements in PGA that describe the motion of a moving frame associated with a parametric curve. We begin by defining *Local Motion Rotors* (LMR), which are rotors that perform a motion that matches the local features of a specified parametric curve at a particular moment in time. An LMR is not necessarily unique. The motivation for creating LMRs is two-fold:

- given a frame associated with a curve, we can specify the motion of the frame at that instance in time in the language of PGA, and
- we can apply the rotors incrementally to recreate the motion of the frame.

To further justify the motivation of creating an LMR, consider a real function $f(t) : \mathbb{R} \rightarrow \mathbb{R}$. The derivative $f'(t)$ specifies the direction of motion of the point $f(t)$. Furthermore, the derivative is associated with a tangent line $l_1(\Delta) = f(t) + \Delta f'(t)$, which is a line that matches local features for the curve f at t . In essence, the element $f'(t)$ is an element representing the local motion of the curve f at t , and it is associated with a transformation of the point $f(t)$ (the translation motion of $l_1(\Delta)$). We could also create a parabola that matches local features of the curve $f(t)$:

$$l_2(\Delta) = f(t) + \Delta f'(t) + \Delta^2 f''(t)/2,$$

and similarly we can create functions $l_k(\Delta)$ to match the local features of $f(t)$ for any $k \geq 0$, where

$$l_k^{(i)}(0) = f^{(i)}(t) \quad \text{for all } i = 0, \dots, k.$$

Similarly to the derivative representing the motion of a function, we want to create an analogous rigid-body motion representation of the motion of a parameterized curve in PGA. Since PGA rotors represent rigid-body motions, we are able to create rotors that perform

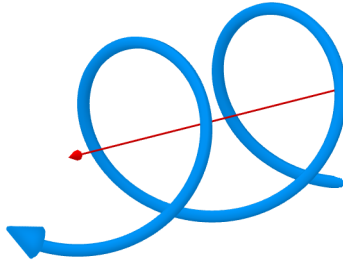


Figure 3.1: A depiction of a screw motion. The red arrow indicates the direction of translation. The blue arrow indicates the screw motion caused by the translation and a perpendicular rotation occurring clock-wise.

rotations and translations, and combinations of these transformations. All rotors in PGA contain a rotation component and a perpendicular translation component. In essence, every rotor specifies a *screw motion*, which is a transformation that performs translation down a line while rotating around the line. See Figure 3.1 for an illustration. Since rotors specify a screw motion, we can specify

- motions with zero curvature (translation). Hence, we can create a rotor that performs a motion analogous to $l_1(\Delta)$, and
- motions with constant non-zero curvature (rotations). Hence, we can create a rotor that moves a point along a path with a particular curvature.

We begin by formally defining LMRs, k th order LMR functions and k th order Local Motion Rotor Exponent (LMRE) functions in Section 3.1. We then derive the first order LMRE function for a parameterized curve f in PGA. The derivation of the second order LMRE function is done in Chapter 4.

3.1 Definitions

Assume we are given a function f that maps a real value $t \in \mathbb{R}$ to a finite point in the affine hyperplane in an n -dimensional PGA,

$$f(t) = f_{\bullet}(t) + \mathbf{e}_0$$

for some function f_{\bullet} that maps $t \in \mathbb{R}$ to a Euclidean vector. Given a rotor R and a vector p directly representing a point, we define the parameterized curve for R and p as

$$\underline{P}_{(R,p)}(\Delta) := R^{\Delta/2} \underline{p} R^{-\Delta/2}.$$

In essence, the function $P_{(R,p)}$ creates a parameterized curve from a rotor R and p , the direct representation of a point. The function $P_{(R,p)}$ is analogous to the functions $l_k(t)$. We say that function $R(t)$ mapping a real value t to a rotor is an *kth order Local Motion Rotor (LMR) function* of f if

$$\begin{aligned} f(t) &= P_{(R(t),f(t))}(0) \\ f(t)' &= P'_{(R(t),f(t))}(0) \\ &\vdots \\ f(t)^{(k)} &= P^{(k)}_{(R(t),f(t))}(0). \end{aligned}$$

Hence, a k th order LMR function $R(t)$ creates a rotor that matches the motion (to the k th-degree) of $f(t)$ at time t . Note that such a function is not always unique and can only exist if f is k times differentiable. Although the definition of an LMR function focuses on the effects of the rotor on a point of the curve f , the rotors created by LMR functions can be applied to any element in the scene to transform the scene.

We are interested in rotors of the form $e^{r(t)}$ where $r(t)$ maps a real number t to a bivector. Thus, if $e^{r(t)}$ is a k th order LMR, we will call $r(t)$ a *kth order Local Motion Rotor Exponent (LMRE) function*.

In this chapter we discuss the case where f is differentiable, but not necessarily twice differentiable. In this case, a natural construction of a first order LMR function is one that translates the point in the direction of f' . Such a first order LMR function is described in the next section.

3.2 Translation Frame

Assuming that f is differentiable, the derivative of f is

$$f'(t) = f'_1(t)\mathbf{e}_1 + f'_2(t)\mathbf{e}_2 + \dots + f'_n(t)\mathbf{e}_n.$$

Since this vector does not have an \mathbf{e}_0 term, $f'(t)$ is purely Euclidean, i.e., $f'(t)$ represents a direction and a magnitude. If we wish to create a rotor for time t that moves the point $f(t)$ in the direction and magnitude $f'(t)$, it suffices to create the LMRE function

$$r_T(t) := f'(t) \wedge \mathbf{e}_0 = f'(t)\mathbf{e}_0. \quad (3.1)$$

Finally, notice that since magnitude of the translation will be $\|f'\|$ and the direction of translation will be f' , the rotor naturally increases and decreases the translation based on the speed in which the point is translating along the curve.

Note that the LMRE function of Equation 3.1 only moves the point of origin via translation and never performs rotation. Hence, the resulting moving frame is the translation frame described in Section 2.6.1. See Figure 3.2 for a comparison with second degree LMRs.

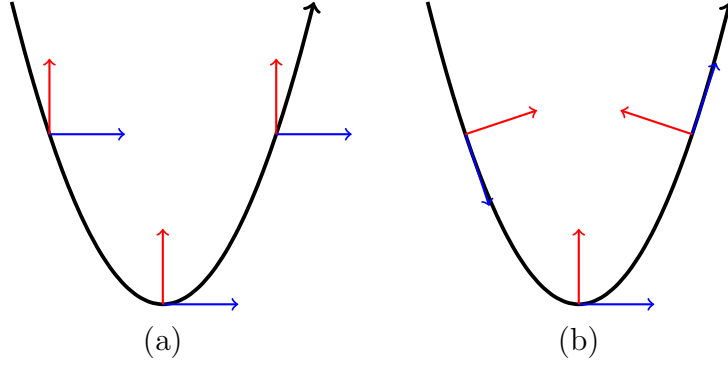


Figure 3.2: A depiction of the differing effects of a first degree LMR and second degree LMR. The parameterized curve is a parabola. (a) A first-degree LMR is applied incrementally with small Δ . (b) A second-degree LMR is applied incrementally with small Δ . For (a) and (b), the frame is depicted at three moments in time.

3.3 Translation Frame Example

Consider the function

$$f(t) = t\mathbf{e}_1 + (t^2 + t)\mathbf{e}_2 + \mathbf{e}_0.$$

The derivative of f is

$$f'(t) = \mathbf{e}_1 + (2t + 1)\mathbf{e}_2,$$

and thus we can construct the rotor at $t = 0$ as

$$\exp(f'(0)\mathbf{e}_0) = \exp((\mathbf{e}_1 + \mathbf{e}_2)\mathbf{e}_0). \quad (3.2)$$

Applying this rotor to the dual representation of the point represented by $f(0) = \mathbf{e}_0$, we get

$$\exp\left(\frac{\Delta}{2}(\mathbf{e}_1 + \mathbf{e}_2)\mathbf{e}_0\right) \underline{\mathbf{e}_0} \exp\left(-\frac{\Delta}{2}(\mathbf{e}_1 + \mathbf{e}_2)\mathbf{e}_0\right) = \underline{\mathbf{e}_0} + \Delta(\underline{\mathbf{e}_1 + \mathbf{e}_2})$$

We see that the parameterized curve from the LMR function is

$$P_{(e^{(\mathbf{e}_1 + \mathbf{e}_2)\mathbf{e}_0}, f(0))}(\Delta) = \mathbf{e}_0 + \Delta(\mathbf{e}_1 + \mathbf{e}_2).$$

Thus, the rotor creates a transformation that corresponds to the tangent line at $t = 0$. See Figure 3.3 for a depiction of applying the rotor for $t = 0$ with $\Delta = 1$ to several points in a scene.

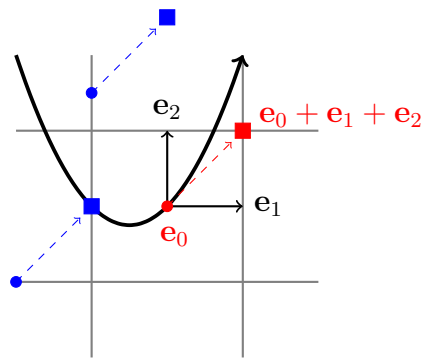


Figure 3.3: A depiction of the effects of the LMR for $t = 0$ for the function $f(t) = t\mathbf{e}_1 + (t^2 + t)\mathbf{e}_2 + \mathbf{e}_0$. The parabola in black is the function $f(t)$ for $-2 \leq t \leq 1$. The entire scene exists in the affine hyperplane. The red circle is the point $f(0) = \mathbf{e}_0$ and the blue circles are other points in the scene. The squares are the points after being transformed by the rotor $\exp(f'(0) \mathbf{e}_0)$ setting $\Delta = 1$. The red square is $\mathbf{e}_0 + \mathbf{e}_1 + \mathbf{e}_2$.

Chapter 4

Second Order Local Motion Rotors

We now assume that f is a twice differentiable function that maps a real value $s \in \mathbb{R}$ to a direct representation of a finite point. To construct a second order LMRE we want to construct a rotor exponent $r(s)$ that, when applied in versor form

$$e^{\Delta/2 \cdot r(s)} \underline{f(s)} e^{-\Delta/2 \cdot r(s)}$$

produces a motion of arc length Δ with velocity $f'(s)$ and local curvature $f''(s)$. In essence, we want to create a rotor exponent that performs a rigid body transformation matching the local curvature of the curve f at s . In particular, if we observe the motion of the point f caused by the rotor, if $f''(s)$ is non-zero, we expect the path of the motion to trace out the osculating circle of the path at that point. If we restrict the rotor to be a rotation in the osculating plane, then the rotor exponent is unique. Furthermore, the corresponding frame for this LMRE function will be the Bishop frame. If we allow the rotor to incorporate other rigid body motions, then those motions must be rotations fixing f at s and rotating perpendicular to \mathbf{T} . In 3D PGA, this restricts the motion to be a rotation in the Euclidean plane that is dual to $f \wedge \mathbf{T}$. The rotation in this plane is referred to as *torsion* and its angle is denoted τ . In higher dimensions, the space of possible rotations is larger and thus torsive movements can be compositions of many independent rotations perpendicular to $f \wedge \mathbf{T}$.

4.1 Constraints on $f(s)$

We pose three constraints on the function f . First, we require that the points created by f are in the affine hyperplane, and hence the \mathbf{e}_0 component of $f(s)$ has the coefficient 1 for all values of s . Thus, f is of the form

$$f(s) = f_{\bullet}(s) + \mathbf{e}_0$$

for some function $f_{\bullet}(s)$ that maps a real number $s \in \mathbb{R}$ to a Euclidean vector. Second, we require that f is twice differentiable, and thus f_{\bullet} is twice differentiable and we have

$$f'(s) = f'_{\bullet}(s), \text{ and}$$

$$f''(s) = f''_{\bullet}(s).$$

Third, to simplify discussion we will require f to be parameterized by arc length [22]. Thus, $\|f'(s)\| = 1$. This third restriction is the motivation for using the parameter variable s instead of t . We use s to emphasize that the parameter is arc length rather than time. We discuss removing this restriction in Section 4.5.

In summary, we require:

1. $f(s) = f_{\bullet}(s) + \mathbf{e}_0$
2. $f(s)$ is twice differentiable at s
3. $\|f'(s)\| = 1$.

4.2 Bishop Frame

We begin by constructing the second order LMRE function that corresponds to the Bishop frame. The Bishop frame is the naturally occurring frame when restricting the rotor to only perform motions in the osculating plane. Unlike the Frenet-Serret frame, the Bishop frame is well-defined everywhere, even at locations of the curve where there is no curvature. However, unlike the Frenet-Serret frame, the Bishop frame at s does not solely depend on the local features of the curve at s . Instead, the Bishop frame is dependent on the starting frame position and the accumulation of rotor effects on the frame from time 0 to s . However, the Bishop frame's local motion at a particular instance in time does *not* depend on these accumulating effects.

The starting frame of the Bishop frame simply requires the origin to be $f(0)$ and for the forward direction to be \mathbf{T} . The other two directions of the frame's basis can be chosen arbitrarily. To allow for the Bishop frame to be easily compared to the Frenet-Serret frame, we will typically set the remaining basis vectors to be \mathbf{N} and \mathbf{B} , though notice that this is not always a viable strategy since the \mathbf{N} and \mathbf{B} may not be well-defined when $s = 0$.

4.2.1 3D Bishop Frame via the Frenet-Serret Formulas

For 3D parameterized curves, we will construct the second order LMRE function $r_B(s)$ by determining the osculating circle of the curve at time s , and then performing the rotation corresponding to the osculating circle in the direction of \mathbf{T} .

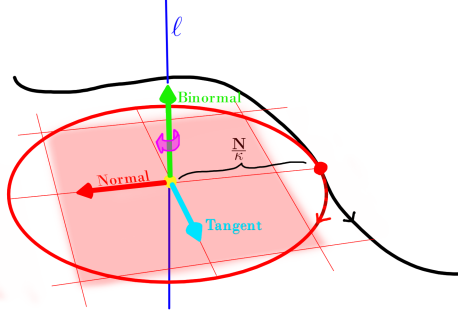


Figure 4.1: A depiction of the line intersecting the osculating circle's center. The black line is the parametric curve. The red circle is the osculating circle. The faint red grid is the osculating plane. The blue arrow is the tangent vector, the red arrow is the normal vector and the green arrow is the binormal vector. The purple arrow depicts the rotation in the osculating plane. The red dot on the curve is the point f . The yellow dot at the center of the osculating circle is the point $f + \mathbf{N}/\kappa$. The dark blue line is the line $(f + \mathbf{N}/\kappa) \wedge \mathbf{B}$.

We begin our construction by using Frenet-Serret formulas. In particular, we have

$$\begin{aligned}\mathbf{T} &= \frac{f'}{\|f'\|} \\ \kappa &= \|\mathbf{T}'\| \\ \mathbf{N} &= \frac{\mathbf{T}'}{\|\mathbf{T}'\|} = \frac{\mathbf{T}'}{\kappa} \\ \mathbf{B} &= \mathbf{T} \times \mathbf{N}.\end{aligned}$$

Note that the values of \mathbf{N} and \mathbf{B} are undefined when $\kappa = 0$. Thus, the first construction we will create for the Bishop frame LMRE function will fail when $\kappa = 0$. In Section 4.2.2 we will show how to remove the dependency on \mathbf{N} and \mathbf{B} to have a second order LMRE function that is well-defined for all values of κ .

Creating a rotor by exponentiating the *dual* of a line creates a rotor that performs a rotation around the line [6]. Thus, we will begin by constructing a line ℓ around which the rotation takes place. See Figure 4.1 for an illustration. The centre of the circle of rotation must be in the direction \mathbf{N} with respect to the point $f(s)$. The radius of the circle must be inversely proportional to the curvature, κ , hence the distance from the point $f(s)$ of the line must be $1/\kappa$ [22]. Thus, we see that the point on the line of rotation ℓ that intersects the osculating plane is

$$f + \frac{\mathbf{N}}{\kappa}.$$

The osculating plane is simply the plane spanned by the vectors \mathbf{N} and \mathbf{T} . Hence, we see that the line of rotation must point in the direction perpendicular to both \mathbf{N} and \mathbf{T} , i.e.,

the line of rotation must point in direction \mathbf{B} . To create the line through point $f + \mathbf{N}/\kappa$ and that points in the direction of \mathbf{B} , it suffices to take the exterior product of both components, giving

$$\underline{\ell} = \left(f + \frac{\mathbf{N}}{\kappa} \right) \wedge \mathbf{B}.$$

We now want to create the rotor exponent that performs the rotation around this line that moves $f(s)$ by the distance Δ in the direction of \mathbf{T} . We have that

$$(\underline{\ell})^2 = -1,$$

the proof of which is in Appendix A. Thus, the rotor that performs a rotation of angle θ around line $\underline{\ell}$ is

$$\exp\left(\frac{\theta}{2} \underline{\ell}\right) = \cos\left(\frac{\theta}{2}\right) + \underline{\ell} \sin\left(\frac{\theta}{2}\right).$$

We want the distance travelled for $f(s)$ to be Δ . Since the radius of the osculating circle is $1/\kappa$, the angle of rotation must be $\theta = \Delta\kappa$ to create a total distance travelled of $(1/\kappa)\theta = \Delta$. Thus we have the rotor

$$\exp\left(\frac{\Delta}{2} r_B\right) = \exp\left(\frac{\Delta}{2} \kappa \underline{\ell}\right) = \cos\left(\frac{\Delta\kappa}{2}\right) + \underline{\ell} \sin\left(\frac{\Delta\kappa}{2}\right)$$

and thus the LMRE function is

$$r_B(s) = \kappa(s) \underline{\ell}(s) \tag{4.1}$$

where

$$\begin{aligned} \kappa(s) &= \|\mathbf{T}'(s)\| \\ \underline{\ell}(s) &= \left(f(s) + \frac{\mathbf{N}(s)}{\kappa(s)} \right) \wedge \mathbf{B}(s). \end{aligned} \tag{4.2}$$

4.2.2 Bishop Frame in terms of f and \mathbf{T}

Recall that since \mathbf{N} and \mathbf{B} do not exist when $\kappa = 0$ (i.e., there is no curvature), the line $\underline{\ell}$ and thus the rotor exponent in Equation 4.1 cannot be computed for values of s when $f(s)$ has no curvature. To ensure the rotor exponent equation can always be evaluated, we will instead construct $r_B(s)$ as the complement of a weighted line. The weighted line will be a line in finite space when $\kappa \neq 0$ and a line at infinity when $\kappa = 0$. When the curvature is non-zero, the rotor exponent created from the following approach will be equivalent to the rotor exponent in Equation 4.1.

We begin by noting that when $\kappa \neq 0$ we have

$$\begin{aligned}
\kappa \ell &= \kappa \left(f + \frac{\mathbf{N}}{\kappa} \right) \wedge \mathbf{B} \\
&= (\kappa f + \mathbf{N}) \wedge \mathbf{B} \\
&= \kappa f \wedge \mathbf{B} + \mathbf{N} \wedge \mathbf{B} \\
&= f \wedge (\kappa \mathbf{B}) + \mathbf{N} \wedge \mathbf{B} \\
&= f \wedge (\kappa \mathbf{T} \times \mathbf{N}) + \mathbf{N} \wedge \mathbf{B} \\
&= f \wedge \left(\kappa \mathbf{T} \times \frac{\mathbf{T}'}{\kappa} \right) + \mathbf{N} \wedge \mathbf{B} \\
&= f \wedge (\mathbf{T} \times \mathbf{T}') + \mathbf{N} \wedge \mathbf{B}.
\end{aligned} \tag{4.3}$$

We can now rewrite Equation 4.3 in terms of derivatives rather than the Frenet-Serret formulas. We notice that $\mathbf{N} \wedge \mathbf{B}$ is precisely the unit 2-blade that is the Euclidean dual to \mathbf{T} . Thus, the value $\mathbf{N} \wedge \mathbf{B}$ can be computed as

$$\mathbf{N} \wedge \mathbf{B} = \overline{\mathbf{T} \wedge \mathbf{e}_0} = \overline{\mathbf{T} \mathbf{e}_0}.$$

Note that the cross product $\mathbf{T} \times \mathbf{T}'$ is the Euclidean dual of their exterior product. Thus we have

$$\mathbf{T} \times \mathbf{T}' = \overline{\mathbf{T}' \wedge \mathbf{T} \wedge \mathbf{e}_0} = \overline{\mathbf{T}' \mathbf{T} \mathbf{e}_0}.$$

Hence, when $\kappa \neq 0$ we have

$$\kappa \ell = f \wedge \overline{\mathbf{T}' \mathbf{T} \mathbf{e}_0} + \overline{\mathbf{T} \mathbf{e}_0}$$

and thus

$$\kappa \underline{\ell} = \underline{f} \vee (\mathbf{T}' \mathbf{T} \mathbf{e}_0) + \mathbf{T} \mathbf{e}_0. \tag{4.4}$$

We can now construct the rotor exponent as

$$r_B = \underline{f} \vee (\mathbf{T}' \mathbf{T} \mathbf{e}_0) + \mathbf{T} \mathbf{e}_0. \tag{4.5}$$

This alternative formulation is equivalent to our previous formulation when $\kappa \neq 0$ since $r_B = \kappa \underline{\ell}$ whenever $\kappa \neq 0$. However, notice that this alternative formulation is well-defined when there is no curvature, since it never divides by κ . When f is parameterized by arc length and $\kappa = 0$, we have $\mathbf{T} = f'$ and $\mathbf{T}' = 0$ and Equation 4.5 simplifies to

$$r_B = f' \mathbf{e}_0. \tag{r_B when \kappa = 0}$$

In essence, when the curvature is zero, we get the rotor exponent performing translation of Equation 3.1.

Hence, we see that the rotor that results from the rotor exponent of Equation 4.5 performs a translation in the degenerate case. The transformation in the degenerate case corresponds to the limit of the transformation of rotating around the osculating circle as the radius approaches infinity. In essence, when the curvature approaches zero, the osculating circle flattens to a line, leading to a translating transformation.

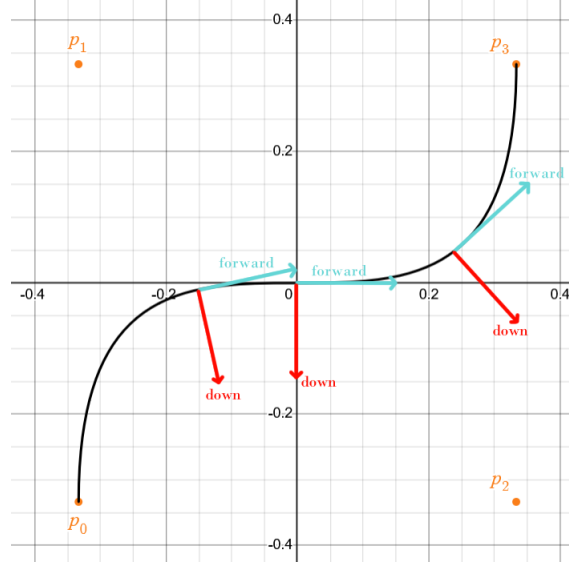


Figure 4.2: A cubic Bézier curve with control points $p_0 = \frac{-\mathbf{e}_1 - \mathbf{e}_2}{3} + \mathbf{e}_0$, $p_1 = \frac{-\mathbf{e}_1 + \mathbf{e}_2}{3} + \mathbf{e}_0$, $p_2 = \frac{\mathbf{e}_1 - \mathbf{e}_2}{3} + \mathbf{e}_0$, and $p_3 = \frac{\mathbf{e}_1 + \mathbf{e}_2}{3} + \mathbf{e}_0$. This figure depicts the affine hyperplane. That is to say, every point on the grid implicitly has a coefficient 1 for the \mathbf{e}_0 term. At three instances in time, the Bishop frame's forward direction and downward direction are illustrated.

4.2.3 Bishop Frame Example

We consider the case of the parametric curve being a cubic Bézier curve. We use this example to illustrate how the Bishop frame LMR is well-defined even when the curvature is zero. Reparameterizing a Bézier curve is difficult [3], thus we intentionally demonstrate a Bézier curve f with the property that at the time of interest $t = 1/2$, we have $\|f'(1/2)\| = 1$ and $f''(1/2) = 0$. To see a discussion of the non-arc length parameterized case, see Section 4.5.

A degree k Bézier curve is a polynomial with $k + 1$ control points p_0, \dots, p_k [9] such that

$$f(t) = \sum_{i=0}^k p_i B_i^k(t)$$

where

$$B_i^k(t) = \binom{k}{i} (1-t)^{k-i} t^i.$$

We choose a degree 3 Bézier curve with control points

$$\begin{aligned} p_0 &= \frac{-\mathbf{e}_1 - \mathbf{e}_2}{3} + \mathbf{e}_0 & p_1 &= \frac{-\mathbf{e}_1 + \mathbf{e}_2}{3} + \mathbf{e}_0 \\ p_2 &= \frac{\mathbf{e}_1 - \mathbf{e}_2}{3} + \mathbf{e}_0 & p_3 &= \frac{\mathbf{e}_1 + \mathbf{e}_2}{3} + \mathbf{e}_0, \end{aligned}$$

as shown in Figure 4.2. The derivative and second derivative of f [9] are

$$f'(t) = 3 \sum_{i=0}^2 (p_{i+1} - p_i) B_i^2(t)$$

$$f''(t) = 6 \sum_{i=0}^1 (p_{i+2} - 2p_{i+1} + p_i) B_i^1(t).$$

Setting $t = 1/2$ we get

$$f(1/2) = \mathbf{e}_0$$

$$f'(1/2) = \mathbf{e}_1$$

$$f''(1/2) = 0.$$

Therefore, $\|f''(1/2)\| = 1$ and $f''(1/2) = 0$ as desired. Hence the LMRE for f at $1/2$ is

$$r_B = f' \mathbf{e}_0 = \mathbf{e}_{10}.$$

This LMRE corresponds to a rotor that performs translation in the \mathbf{e}_1 direction. This matches the expected transformation for when the curvature is zero and the derivative at $t = 1/2$ is $f'(1/2) = \mathbf{e}_1$.

4.3 The Frenet-Serret Frame

To compute the LMRE function for the Frenet-Serret frame, we must incorporate torsion into our instantaneous motion. The torsive movement is a rotation about the tangent vector that rotates the space in accordance to the rate at which the osculating plane is rotating. To construct the rotor for the Frenet-Serret frame, we require the three constraints of Section 4.1 but further require that $f(s)$ is *thrice* differentiable.

We denote the LMRE function for the Frenet-Serret frame as $r_F(s)$. The rotor of this function must incorporate the rotation in the osculating plane and the torsive rotation into one motion. The movement in the osculating plane is identical to that of the Bishop frame, that is, $r_B(s)$. The exponent for the torsive movement we will call $r_\tau(s)$. To incorporate the osculating plane movement $r_B(s)$ and the torsive movement $r_\tau(s)$ into a single movement, we use the Lie product formula. Thus, we can combine the rotor exponents $r_B(s)$ and $r_\tau(s)$ to create $r_F(s) = r_B(s) + r_\tau(s)$ to perform both motions simultaneously. Hence, to derive $r_F(s)$ it suffices now to create $r_\tau(s)$.

To construct $r_\tau(s)$, we assume the vector space's Euclidean subspace is 3-dimensional and that there exists a well-defined Frenet-Serret frame for the curve at s . Therefore, we

know that the osculating plane is rotated around the line $f \wedge \mathbf{T}$ and rotated by the amount τ . Hence, we have the rotor exponent

$$r_\tau = \tau \underline{f \wedge \mathbf{T}} = \tau \underline{f} \vee \underline{\mathbf{T}}. \quad (4.6)$$

This gives us the correct torsive motion at time s .

We now want to combine the motion in the osculating plane defined in Equation 4.5 with the torsive motion defined in Equation 4.6. Recall that by Equation 4.5 we have

$$r_B = \underline{f} \vee (\mathbf{T}'\mathbf{Te}_0) + \mathbf{Te}_0$$

and hence we get

$$\begin{aligned} r_F &= \underline{f} \vee (\mathbf{T}'\mathbf{Te}_0) + \mathbf{Te}_0 + \tau \underline{f} \vee \underline{\mathbf{T}} \\ &= \underline{f} \vee (\mathbf{T}'\mathbf{Te}_0 + \tau \underline{\mathbf{T}}) + \mathbf{Te}_0. \end{aligned} \quad (4.7)$$

We have the following equivalence:

Lemma 4.3.1. *The expression $(\mathbf{T}'\mathbf{Te}_0 + \tau \underline{\mathbf{T}})$ is equivalent to $\underline{\omega}$, the left complement of the Darboux vector $\omega = \tau \mathbf{T} + \kappa \mathbf{B}$.*

Proof. Recall that $\mathbf{T}' = \kappa \mathbf{N}$. Hence, we see that the first term is $\mathbf{T}'\mathbf{Te}_0 = \kappa \mathbf{N}\mathbf{Te}_0$. Furthermore, since \mathbf{T} , \mathbf{N} , \mathbf{B} and \mathbf{e}_0 are all unit and perpendicular, we see that $\mathbf{N}\mathbf{Te}_0 = \underline{\mathbf{T} \times \mathbf{N}} = \underline{\mathbf{B}}$. Hence, we have

$$\mathbf{T}'\mathbf{Te}_0 + \tau \underline{\mathbf{T}} = \kappa \underline{\mathbf{B}} + \tau \underline{\mathbf{T}} = \underline{\omega}.$$

□

Thus we can write

$$r_F = \underline{f} \vee \underline{\omega} + \mathbf{Te}_0 = \underline{f \wedge \omega} + \mathbf{Te}_0. \quad (4.8)$$

4.3.1 Frenet-Serret Frame Example

We consider the case of f being a helix:

$$f(s) = \sin\left(\frac{s}{\sqrt{2}}\right) \mathbf{e}_1 + \cos\left(\frac{s}{\sqrt{2}}\right) \mathbf{e}_2 + \frac{s}{\sqrt{2}} \mathbf{e}_3 + \mathbf{e}_0.$$

We have

$$\begin{aligned} f'(s) &= \frac{\cos\left(\frac{s}{\sqrt{2}}\right) \mathbf{e}_1 - \sin\left(\frac{s}{\sqrt{2}}\right) \mathbf{e}_2 + \mathbf{e}_3}{\sqrt{2}} \\ f''(s) &= \frac{-\sin\left(\frac{s}{\sqrt{2}}\right) \mathbf{e}_1 - \cos\left(\frac{s}{\sqrt{2}}\right) \mathbf{e}_2}{\sqrt{2}}. \end{aligned}$$

It can be shown that $\|f'(s)\| = 1$ for all $s \in \mathbb{R}$ and thus f is parameterized by arc length. Therefore, $\mathbf{T} = f'$ and we have

$$\begin{aligned}\mathbf{T} &= \frac{\cos\left(\frac{s}{\sqrt{2}}\right)\mathbf{e}_1 - \sin\left(\frac{s}{\sqrt{2}}\right)\mathbf{e}_2 + \mathbf{e}_3}{\sqrt{2}} \\ \kappa &= \frac{1}{2} \\ \mathbf{N} &= -\sin\left(\frac{s}{\sqrt{2}}\right)\mathbf{e}_1 - \cos\left(\frac{s}{\sqrt{2}}\right)\mathbf{e}_2 \\ \mathbf{B} &= \frac{\cos\left(\frac{s}{\sqrt{2}}\right)\mathbf{e}_1 - \sin\left(\frac{s}{\sqrt{2}}\right)\mathbf{e}_2 - \mathbf{e}_3}{\sqrt{2}}\end{aligned}$$

and additionally we have

$$\mathbf{B}' = \frac{-\sin\left(\frac{s}{\sqrt{2}}\right)\mathbf{e}_1 - \cos\left(\frac{s}{\sqrt{2}}\right)\mathbf{e}_2}{2} = \frac{1}{2}\mathbf{N}$$

and hence we see that

$$\tau = -\mathbf{N} \cdot \left(\frac{1}{2}\mathbf{N}\right) = -\frac{1}{2}.$$

Finally, this gives us the Darboux vector

$$\begin{aligned}\omega &= \tau\mathbf{T} + \kappa\mathbf{B} \\ &= \left(-\frac{1}{2}\right) \left(\frac{\cos\left(\frac{s}{\sqrt{2}}\right)\mathbf{e}_1 - \sin\left(\frac{s}{\sqrt{2}}\right)\mathbf{e}_2 + \mathbf{e}_3}{\sqrt{2}}\right) + \left(\frac{1}{2}\right) \left(\frac{\cos\left(\frac{s}{\sqrt{2}}\right)\mathbf{e}_1 - \sin\left(\frac{s}{\sqrt{2}}\right)\mathbf{e}_2 - \mathbf{e}_3}{\sqrt{2}}\right) \\ &= -\frac{\mathbf{e}_3}{\sqrt{2}}.\end{aligned}$$

We can thus compute the rotor exponent as

$$\begin{aligned}r_F &= \underline{f \wedge \omega} + \mathbf{T}\mathbf{e}_0 \\ &= \frac{1}{\sqrt{2}} \left(-\sin\left(\frac{s}{\sqrt{2}}\right)\mathbf{e}_{02} + \mathbf{e}_{12} - \sin\left(\frac{s}{\sqrt{2}}\right)\mathbf{e}_{10} + \mathbf{e}_{30}\right).\end{aligned}$$

The full derivation of r_F can be found in [Appendix B](#).

4.4 Comparison of the Three Frames

To compare the translation frame, Bishop frame, and Frenet-Serret frame, we observe their behaviour for the example of Section 4.3.1. The LMRE for the translation frame is

$$r_T = f' \mathbf{e}_0 = \frac{\cos\left(\frac{s}{\sqrt{2}}\right) \mathbf{e}_{10} - \sin\left(\frac{s}{\sqrt{2}}\right) \mathbf{e}_{20} + \mathbf{e}_{30}}{\sqrt{2}}$$

and letting $\theta = s/\sqrt{2}$, the Bishop frame's LMRE is

$$r_B = \frac{1}{2\sqrt{2}} \left(\theta \sin \theta \mathbf{e}_{10} + -\theta \sin \theta \mathbf{e}_{20} - \cos \theta \mathbf{e}_{23} - \sin \theta \mathbf{e}_{13} + \mathbf{e}_{12} \right).$$

The full derivation of r_B can be found in Appendix C.

In Figure 4.3, we show the result of performing small iterations of the LMR for the translation frame, Bishop frame and Frenet-Serret frame. In Figure 4.4, we show how small iterations of the LMR can be used to create a tube around a curve for the translation frame, Bishop frame and Frenet-Serret frame. In both figures, the parameterized curve is $f(s) = \sin(s/\sqrt{2}) \mathbf{e}_1 + \cos(s/\sqrt{2}) \mathbf{e}_2 + (s/\sqrt{2}) \mathbf{e}_3 + \mathbf{e}_0$. For each frame, the starting frame has the origin $f(0)$ and basis vectors $(\mathbf{T}(0), \mathbf{N}(0), \mathbf{B}(0))$. The rotor for each frame is applied incrementally with $\Delta = \sqrt{2} \frac{2\pi}{50}$ to starting points $a_0 = f(0)$, $b_0 = f(0) + \mathbf{N}$ and $c_0 = f(0) + \mathbf{B}$.

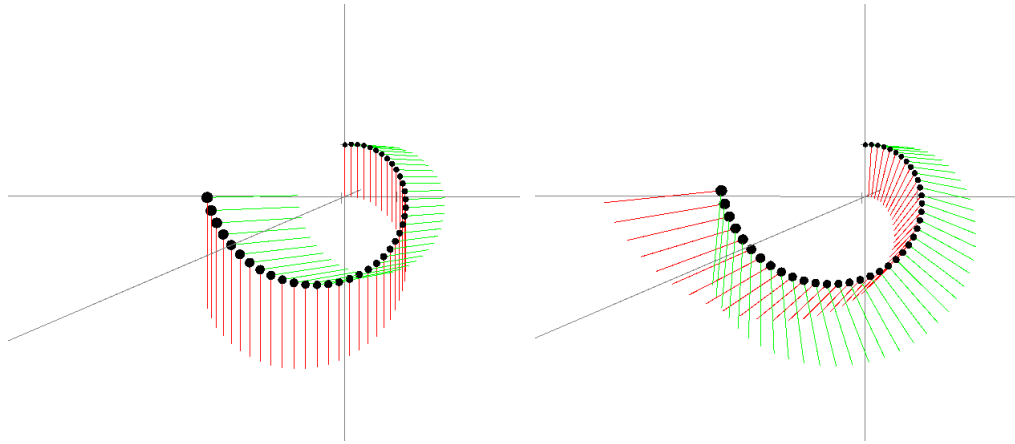
We notice that since the translation frame does not rotate, the construction of a tube around a curve using the translation frame's LMR can result in the tube being squished as in Figure 4.4 (b). The introduction of torsion to create the Frenet-Serret frame from the Bishop frame causes the tube to twist more than the Bishop frame, as can be seen when comparing Figure 4.4 (c) to (d).

4.4.1 Frenet-Serret Frame at Zero Curvature

We note that the Frenet-Serret frame fundamentally breaks when $\kappa = 0$. That is to say, it is generally not possible to consider times when $\kappa = 0$ as removable discontinuities while maintaining the frame. For example, consider the Bézier curve from Section 4.2.3. Here we have

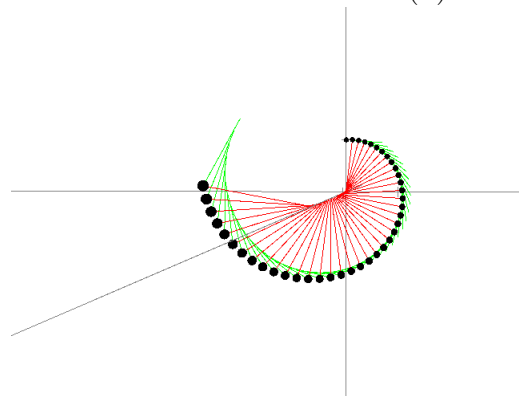
$$\begin{aligned} \lim_{t \rightarrow 1/2^-} \mathbf{N}(s) &= -\mathbf{e}_1 \\ \lim_{t \rightarrow 1/2^+} \mathbf{N}(s) &= \mathbf{e}_1. \end{aligned}$$

Thus, in an n -dimensional space with $n > 2$, the torsive movement would have to instantly rotate the frame by π radians. It is not possible to apply such a rotation instantaneously.



(a) Translation Frame

(b) Bishop Frame



(c) Frenet-Serret Frame

Figure 4.3: A comparison of (a) the translation frame (b) the Bishop frame and (c) the Frenet-Serret frame. At each step $i = 1, \dots, 40$, the frame's origin (a_i) is drawn as a black dot, the down direction (a_i to b_i) is drawn as a red line and the left direction (a_i to c_i) is drawn as a green line. In the case of (c) the Frenet-Serret frame, the red lines correspond to the normal and the green lines correspond to the binormal.

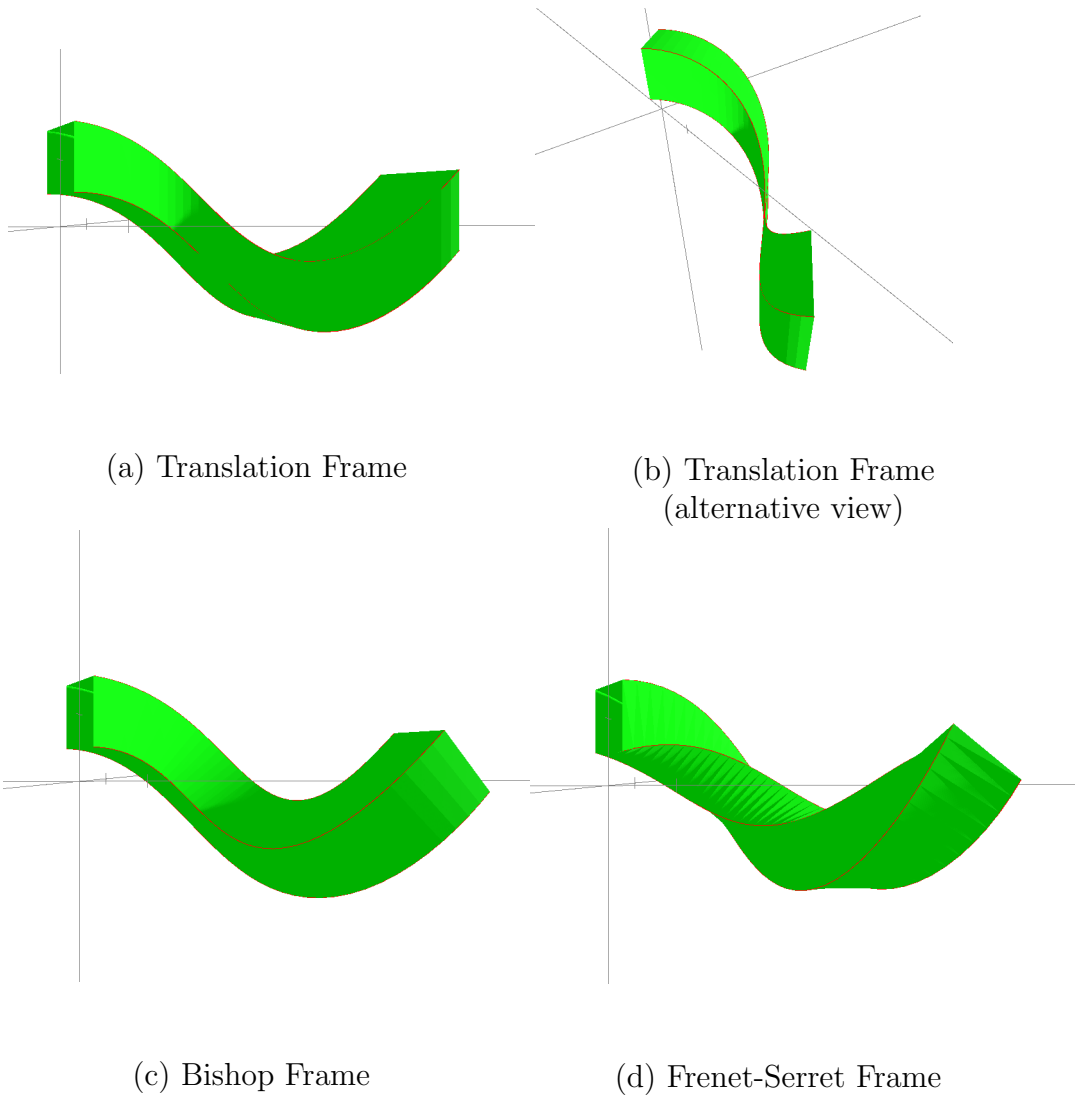


Figure 4.4: A comparison of tubes constructed via (a), (b) the translation frame (c) the Bishop frame and (d) the Frenet-Serret frame. At each step $i = 1, \dots, 40$, for each pair $(v, w) = (a, b), (b, c), (c, d), (d, a)$ a green square with corners $w_{i-1}, w_i, v_i, v_{i-1}$ and a red line v_{i-1} to v_i is drawn.

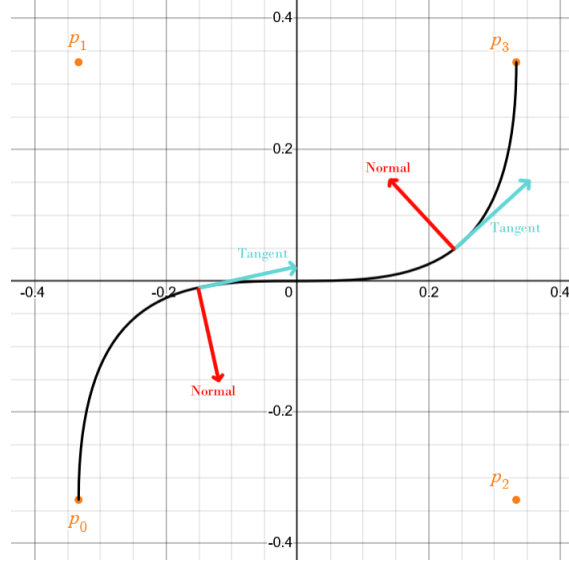


Figure 4.5: A cubic Bézier curve with control points $p_0 = \frac{-\mathbf{e}_1 - \mathbf{e}_2}{3} + \mathbf{e}_0$, $p_1 = \frac{-\mathbf{e}_1 + \mathbf{e}_2}{3} + \mathbf{e}_0$, $p_2 = \frac{\mathbf{e}_1 - \mathbf{e}_2}{3} + \mathbf{e}_0$, and $p_3 = \frac{\mathbf{e}_1 + \mathbf{e}_2}{3} + \mathbf{e}_0$. This figure depicts the affine hyperplane. That is to say, every point on the grid implicitly has a coefficient 1 for the \mathbf{e}_0 term. At two instances in time, the Frenet-Serret frame's forward direction, the tangent, and downward direction, the normal, are illustrated.

In a 2-dimensional space, the reflection of \mathbf{N} leads to a configuration in which no rigid-body transformation can transition from one frame to the other. See Figure 4.5 for an illustration. Thus, moments when $\kappa = 0$ are generally not removable discontinuities.

However, if one is simply interested in performing the instantaneous motions associated with the Frenet-Serret frame at times when $\kappa \neq 0$ (while not necessarily maintaining the frame itself), then the instances when $\kappa = 0$ are computable. In particular, notice that when $\tau = 0$ we have

$$r_F = \underline{f} \vee (\mathbf{T}'\mathbf{T}\mathbf{e}_0 + \tau\mathbf{T}) + \mathbf{T}\mathbf{e}_0 = \underline{f} \vee (\mathbf{T}'\mathbf{T}\mathbf{e}_0) + \mathbf{T}\mathbf{e}_0 = r_B.$$

In essence, the Frenet-Serret frame LMR is equivalent to the Bishop frame LMR when torsion is zero. Since the Bishop frame's LMR is well-defined for instances of zero curvature, we can simply set the Frenet-Serret frame's motion to have zero torsion over intervals of zero curvature. However, note that this technique means that the torsive motion will appear to be discontinuous (i.e., it will suddenly stop and start again) unless the curve's torsion already approaches 0 before and after intervals with zero curvature. Additionally, notice that using the Bishop frame rotor to repair instances when $\kappa = 0$ is equivalent to using the translation frame's rotor during these instances. Since we know that $\kappa = 0$ during the intervals where we use the Bishop frame LMR, we have

$$r_B = \underline{f} \vee (\mathbf{T}'\mathbf{T}\mathbf{e}_0) + \mathbf{T}\mathbf{e}_0 = \mathbf{T}\mathbf{e}_0 = f'\mathbf{e}_0 = r_T.$$

Therefore, we are effectively patching the instances where $\kappa = 0$ by using the LMR for the translation frame.

This approach allows us to perform the motions associated with the Frenet-Serret frame and could be used to construct tubes like in Figure 4.4 even when the curvature goes to 0. However, this method does not maintain the Frenet-Serret frame itself. For example, notice that the Bézier curve from Section 4.2.3 exists in a 2D plane, and thus the curve has zero torsion. Therefore, using the Bishop frame LMR effectively fixes the discontinuity at $t = 1/2$. However, the frame after the discontinuity no longer matches the Frenet-Serret frame (in fact, in this case, the patched Frenet-Serret frame approach results in the Bishop frame, see Figure 4.2). Hence, the main disadvantage of this approach is that the Frenet-Serret frame ceases to be maintained after the first discontinuity, i.e., one can no longer determine the non-forward basis vectors based purely on local features of the curve because they are no longer necessarily \mathbf{N} and \mathbf{B} . However, the main advantage is that we maintain the forward direction to be the tangent vector \mathbf{T} and we retain the instantaneous motion of the Frenet-Serret frame at instances with non-zero curvature.

4.5 Non-Arc Length Parameterized Curves

So far we have defined LMRE functions for arc length parameterized curves. However, non-arc length parameterized curves are often used in practice. In the case of the function f being a non-arc length parameterized curve, we can also construct the LMRE functions for the Bishop frame and Frenet-Serret frame. We no longer require $\|f'\| = 1$, however we still require $\|f'\| \neq 0$ since otherwise \mathbf{T} and ω are undefined.

The equation for the Bishop frame, Equation 4.5, can be rewritten as

$$\begin{aligned} r_B &= \|f'\| (\underline{f} \vee (\mathbf{T}' \mathbf{T} \mathbf{e}_0) + \mathbf{T} \mathbf{e}_0) \\ &= \underline{f} \vee (\mathbf{T}' f' \mathbf{e}_0) + f' \mathbf{e}_0. \end{aligned} \tag{4.9}$$

In essence, we can simply multiply by $\|f'\|$ to have the speed of the rotor match f' . Similarly, the equation for the Frenet-Serret frame, Equation 4.8, can be rewritten as

$$\begin{aligned} r_F &= \|f'\| (\underline{f} \wedge \omega + \mathbf{T} \mathbf{e}_0) \\ &= \|f'\| \underline{f} \wedge \omega + f' \mathbf{e}_0. \end{aligned} \tag{4.10}$$

Chapter 5

Higher Dimensional Frames

5.1 Translation Frames and Bishop Frames

Construction of the LMRE functions for translation frames and Bishop frames is relatively simple. For the translation frame, $r(t) = f'(t)\mathbf{e}_0$ remains identical regardless of the dimensionality of the space. For the Bishop frame, the formula

$$r_B(s) = \underline{f} \vee (\mathbf{T}'\mathbf{T}\mathbf{e}_0) + \mathbf{T}\mathbf{e}_0$$

remains identical for higher dimensional spaces. However, note that the left complement operation in \underline{f} results in different elements depending on the dimensionality of the space. The operations differ because increasing the dimensionality of the space changes the pseudoscalar. For example, $\underline{\mathbf{e}}_1 = -\mathbf{e}_2$ in a 2-dimensional space, but $\underline{\mathbf{e}}_1 = \mathbf{e}_{23}$ in a 3-dimensional space.

5.2 Frenet-Serret Frames

Just as how the Frenet-Serret frame is undefined in the 3D case when the curvature is zero, the Frenet-Serret frame is similarly undefined under certain circumstances in the general n -dimensional case. Given a parametric curve in an n -dimensional space that is n -times differentiable, we require that the set of the first n derivatives $\{f', f'', \dots, f^{(n)}\}$ are linearly independent. If that is the case, we can create the Frenet-Serret frame basis vectors by applying the Gram-Schmidt process on the first n derivatives of f [23]. We then normalize this set of vectors to create an orthogonal basis consisting of unit vectors. If the set of derivatives $\{f', f'', \dots, f^{(n)}\}$ is not linearly independent, the Gram-Schmidt process will not yield a valid frame for our n -dimensional space, and so the Frenet-Serret frame is undefined.

After applying the Gram-Schmidt process, we will refer to the resulting unit vectors as $\mathbf{F}_1, \mathbf{F}_2, \dots, \mathbf{F}_n$. The correspondence in the 3D case is

$$\begin{aligned}\mathbf{F}_1 &= \mathbf{T} \\ \mathbf{F}_2 &= \mathbf{N} \\ \mathbf{F}_3 &= \mathbf{B}.\end{aligned}$$

We refer to the basis of the frame as

$$\mathbf{F} = \begin{bmatrix} \mathbf{F}_1 \\ \mathbf{F}_2 \\ \vdots \\ \mathbf{F}_n \end{bmatrix}$$

and then we have the relation that the frame transforms via

$$\mathbf{F}' = K\mathbf{F}$$

where

$$K = \begin{bmatrix} 0 & \kappa_1 & 0 & 0 & \dots & 0 \\ -\kappa_1 & 0 & \kappa_2 & 0 & \dots & 0 \\ 0 & -\kappa_2 & \ddots & \ddots & \ddots & \vdots \\ 0 & 0 & \ddots & \ddots & \ddots & 0 \\ \vdots & \ddots & \ddots & \ddots & 0 & \kappa_{n-1} \\ 0 & \dots & \dots & 0 & -\kappa_{n-1} & 0 \end{bmatrix} \quad (5.1)$$

as described in [23]. In essence, the vector \mathbf{F}_i rotates towards \mathbf{F}_{i+1} by amount κ_i , where $\kappa_i = \|\mathbf{F}'_i\|$. We refer to the plane $\mathbf{F}_{i+1} \wedge \mathbf{F}_i$ as the *ith torsion plane*. Thus, in the 3D case, the osculating plane is the 1st torsion plane and the normal plane is the 2nd torsion plane. These rotations are performed while fixing the point f . Hence, the rotations of the point are described by the rotor exponents

$$\sum_{i=1}^{n-1} \kappa_i \underline{f} \vee (\mathbf{F}_{i+1} \wedge \mathbf{F}_i \wedge \mathbf{e}_0) = \underline{f} \vee \left(\sum_{i=1}^{n-1} \kappa_i \mathbf{F}_{i+1} \wedge \mathbf{F}_i \wedge \mathbf{e}_0 \right).$$

By Equation 5.1, we have that for $1 < i < n$,

$$\mathbf{F}'_i = -\kappa_{i-1} \mathbf{F}_{i-1} + \kappa_i \mathbf{F}_{i+1}$$

and thus we have that

$$\begin{aligned}\mathbf{F}'_i \wedge \mathbf{F}_i &= -\kappa_{i-1} \mathbf{F}_{i-1} \wedge \mathbf{F}_i + \kappa_i \mathbf{F}_{i+1} \wedge \mathbf{F}_i \\ &= \kappa_{i-1} \mathbf{F}_i \wedge \mathbf{F}_{i-1} + \kappa_i \mathbf{F}_{i+1} \wedge \mathbf{F}_i.\end{aligned}$$

Additionally, for $i = 1$ and $i = n$, Equation 5.1 gives us

$$\begin{aligned} F'_1 &= \kappa_1 \mathbf{F}_2 \\ F'_n &= -\kappa_{n-1} \mathbf{F}_{n-1} \end{aligned}$$

and thus

$$\begin{aligned} \mathbf{F}'_1 \wedge \mathbf{F}_1 &= \kappa_1 \mathbf{F}_2 \wedge \mathbf{F}_1 \\ \mathbf{F}'_n \wedge \mathbf{F}_n &= \kappa_{n-1} \mathbf{F}_n \wedge \mathbf{F}_{n-1} \end{aligned}$$

hence, we have that

$$\sum_{i=1}^n \mathbf{F}'_i \wedge \mathbf{F}_i = 2 \sum_{i=1}^n \kappa_i \mathbf{F}_{i+1} \wedge \mathbf{F}_i$$

and therefore the rotor exponent for the instantaneous rotation is

$$\frac{1}{2} \underline{f} \vee \left(\sum_{i=1}^n (\mathbf{F}'_i \wedge \mathbf{F}_i) \wedge \mathbf{e}_0 \right).$$

As before, the rotor exponent for the instantaneous translation is

$$f' \mathbf{e}_0$$

and thus, by the Lie product formula, the rotor exponent describing the entire transformation is

$$\frac{1}{2} \underline{f} \vee \left(\sum_{i=1}^n (\mathbf{F}'_i \wedge \mathbf{F}_i) \wedge \mathbf{e}_0 \right) + f' \mathbf{e}_0.$$

In the 3D case, we see that this is an equivalent result since we have the mapping

$$\begin{aligned} \kappa_1 &= \kappa \\ \kappa_2 &= \tau \end{aligned}$$

and thus we have

$$\begin{aligned} \frac{1}{2} \underline{f} \vee \left(\sum_{i=1}^n (\mathbf{F}'_i \wedge \mathbf{F}_i) \wedge \mathbf{e}_0 \right) + f' \mathbf{e}_0 &= \underline{f} \vee \left(\sum_{i=1}^{n-1} \kappa_i \mathbf{F}_{i+1} \wedge \mathbf{F}_i \wedge \mathbf{e}_0 \right) + f' \mathbf{e}_0 \\ &= \underline{f} \vee (\kappa \mathbf{N} \wedge \mathbf{T} \wedge \mathbf{e}_0 + \tau \mathbf{B} \wedge \mathbf{N} \wedge \mathbf{e}_0) + f' \mathbf{e}_0 \\ &= \underline{f} \vee (\mathbf{T}' \wedge \mathbf{T} \wedge \mathbf{e}_0 + \tau \underline{\mathbf{T}}) + \mathbf{T} \mathbf{e}_0 \\ &= \underline{f} \vee (\mathbf{T}' \mathbf{T} \mathbf{e}_0 + \tau \underline{\mathbf{T}}) + \mathbf{T} \mathbf{e}_0. \end{aligned}$$

which exactly matches Equation 4.7.

5.3 The Darboux Bivector

We can generalize the notion of a Darboux pseudovector in 3D to the case of general dimensions by defining the *Darboux bivector* as

$$\Omega := \frac{1}{2} \sum_{i=1}^n \mathbf{F}'_i \wedge \mathbf{F}_i. \quad (5.2)$$

This bivector represents the rotation of the frame. We can thus rewrite the rotor exponent as

$$\underline{f} \vee (\Omega \wedge \mathbf{e}_0) + f' \mathbf{e}_0.$$

For the 3D case, we have the relation

$$\Omega \wedge \mathbf{e}_0 = \underline{\omega}$$

and hence this is why we can write the 3D case as

$$\underline{f} \vee \underline{\omega} + f' \mathbf{e}_0.$$

Chapter 6

Conclusions

In this thesis, we combined Projective Geometric Algebra with tools from differential geometry to demonstrate how to derive rotors that describe the local motion of frames associated with parametric curves. In particular, we showed how to construct rotors for the translation frame, Bishop frame and Frenet-Serret frame. We then showed how to generalize these results to higher-dimensional spaces. These results further develop intersection of the fields of geometric algebra and differential geometry.

6.1 Contributions

First, standard methods for Frenet-Serret frames and other frames associated with parametric curves tend to use linear algebra instead of geometric algebra. This thesis contributes to the body of literature of PGA by demonstrating how PGA can be used for applications in differential geometry. Furthermore, since the standard approach uses linear algebra instead of PGA, it cannot represent lines and planes offset from the origin. Our formulation of LMRs allow us to apply the rigid-body motions associated with parametric curves to lines and planes as elements of the space.

Additionally, the standard approach typically excludes the transformation of the frame's origin from discussion. Although moving frames correspond to rigid-body motions, the literature normally treats the rotation of the basis vectors of the frame and the translation of the frame's origin separately. Therefore, the derived transformations typically do not model the entire rigid-body transformation, but rather the transformations only capture the transformation of the basis vectors of the frame. Our construction of LMRs includes the entire transformation of the frame as one element. In the case of the Bishop frame, the approach of this thesis effectively handles the case when the curve has zero curvature, where the rotor corresponds to a translation transformation. For the Frenet-Serret frame,

our approach can maintain the frame's origin and tangent vector in the degenerate case of $\kappa = 0$. However, our approach for the degenerate case does not necessarily preserve the normal or binormal vectors of the Frenet-Serret frame. The inability to maintain the normal and binormal vectors in the degenerate case is an inherent limitation of the problem.

The literature typically uses a matrix applied to the frame in the form of a differential equation to describe the local motion of the curve. In particular, given a frame $\mathbf{F} = [\mathbf{F}_1 \ \mathbf{F}_2 \ \dots \ \mathbf{F}_n]^T$ where \mathbf{F}_i are unit vectors representing the basis of the frame, the local motion is defined in the form

$$\mathbf{F}' = M\mathbf{F} \quad (6.1)$$

for some skew-symmetric matrix M . For example, Gökçelik et al. [11] and Ross [23] use this form to generalize Frenet-Serret frames and parallel transport frames to higher-dimensional cases. Equation 5.1 is an example of an equation of the form of Equation 6.1. The PGA approach for the Bishop frame derived in this thesis allows for a “frame-free” description of the local transformation of frame. In essence, it describes the rigid-body motion of the local motion of the curve without referencing a particular frame. In the linear algebra approach, the instantaneous motion of the Bishop frame is normally described [11, 13] by the differential equation

$$\mathbf{F}' = \begin{bmatrix} 0 & \kappa_1 & \kappa_2 & \dots & \kappa_{n-1} \\ -\kappa_1 & & & & \\ \vdots & & & & \\ -\kappa_{n-1} & & & & \end{bmatrix} \mathbf{F}. \quad (6.2)$$

The values κ_i corresponds to $\mathbf{T}' \cdot \mathbf{F}_{i+1}$ [11]. Thus, the choice of the starting frame $\mathbf{F}(0)$ changes the resulting transformation matrices that describe the local motion of the moving frame. Our approach for describing the motion of the Bishop frame by the rotor $r_B = \underline{f} \vee (\mathbf{T}'\mathbf{Te}_0) + \mathbf{Te}_0$ (Equation 4.5) does not reference a particular frame. Thus, we are able to describe the local rigid-body motion of the curve without making an arbitrary choice of a starting frame.

The higher-dimensional approach in PGA for the Frenet-Serret frame does not allow the construction of the rotor to be frame-free. However, the approach of this thesis constructs a higher-dimensional generalization of the Darboux vector, the Darboux bivector. Therefore, we are able to construct an element that describes the instantaneous rotation movement of the Frenet-Serret frame in higher-dimensional spaces.

In summary, this thesis makes the following contributions:

- This thesis contributes to the body of literature establishing the uses of PGA. In particular, it highlights how PGA can be used for differential geometry. Consequently, the PGA approach is easily able to apply the transformations of moving frames to lines and planes.

- Compared to the standard approach, our approach incorporates the entire rigid-body motion of the frame, not just the rotation of the frame. Our approach effectively handles the case where $\kappa = 0$ for the Bishop frame. For the Frenet-Serret frame, our approach manages to preserve the correct origin and tangent vector for the degenerate case $\kappa = 0$.
- Our construction of the Bishop frame rotor does not make reference to a particular frame. Hence, our construction can describe the local rigid-body motion of the frame without choosing a starting frame.
- Our approach with the Frenet-Serret frame generalizes the Darboux vector in spaces with dimensionality larger than 3.

6.2 Future Directions

There are multiple future directions to explore while limiting oneself to using rigid-body motions. One area of research would be to augment the translation frame to allow for user-defined rotations. For example, we could define a point p (either as a finite point or a point at infinity) and have the frame's forward direction point to p as the frame moves down the curve. Maintaining the forward direction to point to p allows for rotations transforming the other basis vectors. Hence, there may be variations of the augmented translation frame that allow for the other basis vectors to have interesting properties.

Another future area of research would be to “integrate” the LMR developed in this thesis. In particular, we could ask how to create a function $B(t)$ that maps $t \in \mathbb{R}$ to a bivector such that

$$\begin{aligned} \exp(B(t)) f(0) \exp(-B(t)) &= f(t) \\ \exp(B(t)) \mathbf{F}_1(0) \exp(-B(t)) &= \mathbf{F}_1(t) \\ &\vdots \\ \exp(B(t)) \mathbf{F}_n(0) \exp(-B(t)) &= \mathbf{F}_n(t), \end{aligned}$$

where \mathbf{F}_i are the basis vectors of the frame. In essence, the function $B(t)$ outputs the bivector that describes the *total* rigid-body transformation from $f(0)$ to $f(t)$.

When limiting oneself to rigid-body motions, the curve $P_{(R,p)}$ created from the rotor R must trace out a path that is a combination of translations and rotations. The translation's distance and rotation's angle increase linearly with the increase of the rotor's exponential, and thus the rotor R performs a screw motion. Screw motions have constant curvature, and thus $P''_{(R,p)} = 0$. Therefore, it is impossible to create a k degree LMR for $k > 2$ for curves with non-zero second derivatives. A future direction of research could be to investigate

non-rigid-body transformations that may be of interest that would allow for higher order agreement. In particular, conformal or hyperbolic transformations may be of interest.

Using other models of geometric algebra to investigate moving frames associated with parametric curves may also be of interest. In particular, the conformal model of geometric algebra allows for the construction of elements that represent circles [17]. Thus, one can construct an element representing the osculating circle, which may have some application in computing LMRs.

References

- [1] Miklós Bergou, Max Wardetzky, Stephen Robinson, Basile Audoly, and Eitan Grinspun. Discrete elastic rods. *ACM Trans. Graph.*, 27(3):1–12, August 2008.
- [2] Richard Bishop. There is More than One Way to Frame a Curve. *The American Mathematical Monthly*, 82:Mathematical Association of America–, 03 1975.
- [3] Norbert Brodtmann and Daniel Schilberg. Dynamic Bézier Curves: New Findings on Reparameterization by Arc length. 01 2022.
- [4] Jiwen Cui, Shiyuan Zhao, Chaoqiang Yang, and Jiubin Tan. Parallel Transport Frame for Fiber Shape Sensing. *IEEE Photonics Journal*, 10(1):1–12, 2018.
- [5] R. W. R. Darling. *Surface Theory Using Moving Frames*, pages 17–20, 76–97. Cambridge University Press, 1994.
- [6] Leo Dorst and Steven De Keninck. *A Guided Tour to the Plane-Based Geometric Algebra PGA*. 2022.
- [7] Tevian Dray. <https://sites.science.oregonstate.edu/~tevian/onid/Courses/MTH434/2009/dual.pdf>, 1999.
- [8] Benson Farb and R. Keith Dennis. *Noncommutative Algebra*, page 13. Springer New York, NY, 2012.
- [9] Gerald Farin. *Curves and Surfaces for CAGD: a Practical Guide*. Morgan Kaufmann Publishers Inc., 5th edition, 2001.
- [10] Charles G. Gunn. Projective geometric algebra: A new framework for doing Euclidean geometry, 2020.
- [11] Fatma Gökçelik, Zehra Bozkurt, İsmail Gök, F. Nejat Ekmekci, and Yusuf Yayli. Parallel Transport Frame in 4-dimensional Euclidean Space, 2012.
- [12] Brian C. Hall. *Lie Groups, Lie Algebras, and Representations*, page 40. Springer Cham, 2015.

- [13] Andrew Hanson. Quaternion Frenet Frames: Making Optimal Tubes and Ribbons from Curves. 08 1994.
- [14] Serge Lang. *Algebra*, page 633. Springer New York, NY, 2002.
- [15] Zachary Leger and Stephen Mann. PGABLE. <https://cs.uwaterloo.ca/~smann/PGABLE/>, 2024.
- [16] Eric Lengyel. *Projective Geometric Algebra Illuminated*. Terathon Software LLC, 2024.
- [17] Leo Dorst, Daniel Fontijne and Stephen Mann. *Geometric Algebra for Computer Science*. Morgan Kaufmann, 2007.
- [18] Yaron Lipman, Daniel Cohen-Or, Ran Gal, and David Levin. Volume and shape preservation via moving frame manipulation. *ACM Trans. Graph.*, 26(1):5–es, January 2007.
- [19] Marjeta Kneza, Francesca Pelosic and Maria Lucia Sampolic. On G2 interpolation by degree seven Minkowski Pythagorean-hodograph spline curves. *Preprint submitted to Elsevier*, 2025.
- [20] Antony Nutbourne and Ralph Martin. *Differential Geometry Applied to Curve and Surface Design*, page 19. Ellis Horwood Limited, 1988.
- [21] Barret O’Neill. *Elementary Differential Geometry*. Academic Press, Inc., 1966.
- [22] Andrew Pressley. *Elementary Differential Geometry*, pages 10–15, 24. Springer London, 2010.
- [23] Catherine Elaina Eudora Ross. The Frenet Frame and Space Curves. Master’s thesis, Missouri State University, 2019.
- [24] Manel Velasco, Isiah Zaplana, Arnau Dòria-Cerezo, and Pau Martí. SUGAR. <https://github.com/distributed-control-systems/SUGAR>, 2025.
- [25] Manel Velasco, Isiah Zaplana, Arnau Dòria-Cerezo, and Pau Martí. Symbolic and User-friendly Geometric Algebra Routines (SUGAR) for Computations in Matlab. *ACM Transactions on Mathematical Software*, 51(2):1–31, June 2025.
- [26] Wenping Wang, Bert Jüttler, Dayue Zheng, and Yang Liu. Computation of rotation minimizing frames. *ACM Trans. Graph.*, 27(1), March 2008.

APPENDICES

Appendix A

Proof of $(\underline{\ell})^2 = -1$

To complete the derivation of the Bishop frame rotor LMRE in Section 4.2.1, we are required to prove $(\underline{\ell})^2 = -1$. We note that since $f = f_{\bullet} + \mathbf{e}_0$ for some function $f_{\bullet}(s)$ mapping a real number s to a Euclidean vector, we have

$$\begin{aligned}\ell &= \left(f + \frac{\mathbf{N}}{\kappa} \right) \wedge \mathbf{B} \\ &= \mathbf{e}_0 \mathbf{B} + f_{\bullet} \wedge \mathbf{B}.\end{aligned}$$

We note that every 2-blade B can be written in terms of vectors a and b such that $B = a \wedge b = ab$. That is, we can factor B in terms of the geometric product of two vectors a and b such that a and b are perpendicular and anticommutative with each other. Thus, for any 2-blade B we have $B^2 = abab = -abba = -Q(a)Q(b)$. In essence, 2-blades square to scalars. Since ℓ is a 2-blade, so is its complement in a 4-dimensional space, and thus $(\underline{\ell})^2$ is a scalar. Expanding $(\underline{\ell})^2$ we get

$$\begin{aligned}(\underline{\ell})^2 &= (\mathbf{e}_0 \mathbf{B} + f_{\bullet} \wedge \mathbf{B})^2 \\ &= (\mathbf{e}_0 \mathbf{B})^2 + (\mathbf{e}_0 \mathbf{B})(f_{\bullet} \wedge \mathbf{B}) + (f_{\bullet} \wedge \mathbf{B})(\mathbf{e}_0 \mathbf{B}) + (f_{\bullet} \wedge \mathbf{B})^2.\end{aligned}$$

We note that the term

$$\underline{f_{\bullet} \wedge \mathbf{B}}$$

must contain a factor of \mathbf{e}_0 since $f_{\bullet} \wedge \mathbf{B}$ is purely Euclidean. This means that $(\underline{f_{\bullet} \wedge \mathbf{B}})^2 = 0$. We now notice that $\underline{\mathbf{e}_0 \mathbf{B}} = \mathbf{N} \mathbf{T}$ and thus

$$(\underline{\mathbf{e}_0 \mathbf{B}})^2 = \mathbf{N} \mathbf{T} \mathbf{N} \mathbf{T} = -\mathbf{N} \mathbf{T} \mathbf{T} \mathbf{N} = -1.$$

Furthermore, notice that the term

$$\underline{\mathbf{e}_0 \mathbf{B}}$$

must *not* contain a factor of \mathbf{e}_0 , since it is the complement of a 2-blade that does. Therefore, the terms

$$(\underline{\mathbf{e}_0 \mathbf{B}})(\underline{f \bullet \wedge B}) \text{ and } (\underline{f \bullet \wedge B})(\underline{\mathbf{e}_0 \mathbf{B}})$$

must contain a factor of \mathbf{e}_0 . Since we know the result of $(\underline{\ell})^2$ is a scalar, this means that the two terms cancel out, leaving us with

$$(\underline{\ell})^2 = -1.$$

Appendix B

Full Derivation of Frenet Frame Example Rotor

We wish to derive the Frenet-Serret frame LMRE in Section 4.3.1. We can compute the rotor exponent as

$$\begin{aligned} r_F &= f \wedge \omega + \mathbf{T}\mathbf{e}_0 \\ &= \left(\sin\left(\frac{s}{\sqrt{2}}\right) \mathbf{e}_1 + \cos\left(\frac{s}{\sqrt{2}}\right) \mathbf{e}_2 + \frac{s}{\sqrt{2}} \mathbf{e}_3 + \mathbf{e}_0 \right) \wedge \left(-\frac{\mathbf{e}_3}{\sqrt{2}} \right) \\ &\quad + \left(\frac{\cos\left(\frac{s}{\sqrt{2}}\right) \mathbf{e}_1 - \sin\left(\frac{s}{\sqrt{2}}\right) \mathbf{e}_2 + \mathbf{e}_3}{\sqrt{2}} \right) \mathbf{e}_0 \\ &= \frac{1}{\sqrt{2}} \left(-\sin\left(\frac{s}{\sqrt{2}}\right) \mathbf{e}_{13} - \cos\left(\frac{s}{\sqrt{2}}\right) \mathbf{e}_{23} - \mathbf{e}_{03} + \cos\left(\frac{s}{\sqrt{2}}\right) \mathbf{e}_{10} - \sin\left(\frac{s}{\sqrt{2}}\right) \mathbf{e}_{10} + \mathbf{e}_{30} \right) \\ &= \frac{1}{\sqrt{2}} \left(-\sin\left(\frac{s}{\sqrt{2}}\right) \mathbf{e}_{02} + \cos\left(\frac{s}{\sqrt{2}}\right) \mathbf{e}_{01} + \mathbf{e}_{12} + \cos\left(\frac{s}{\sqrt{2}}\right) \mathbf{e}_{10} - \sin\left(\frac{s}{\sqrt{2}}\right) \mathbf{e}_{10} + \mathbf{e}_{30} \right) \\ &= \frac{1}{\sqrt{2}} \left(-\sin\left(\frac{s}{\sqrt{2}}\right) \mathbf{e}_{02} + \mathbf{e}_{12} - \sin\left(\frac{s}{\sqrt{2}}\right) \mathbf{e}_{10} + \mathbf{e}_{30} \right). \end{aligned}$$

Appendix C

Full Derivation of Bishop Frame Example Rotor

We wish to derive the Bishop frame LMRE in Section 4.4. We can compute the rotor exponent as

$$\begin{aligned} r_B &= \underline{f} \vee (\mathbf{T}\mathbf{T}'\mathbf{e}_0) + f'\mathbf{e}_0 \\ &= \underline{f \wedge \kappa\mathbf{B}} + r_T. \end{aligned}$$

Since we know

$$r_T = \frac{\cos\left(\frac{s}{\sqrt{2}}\right)\mathbf{e}_{10} - \sin\left(\frac{s}{\sqrt{2}}\right)\mathbf{e}_{20} + \mathbf{e}_{30}}{\sqrt{2}}$$

from Subsection 4.3.1, it suffices to solve $\underline{f \wedge \kappa\mathbf{B}}$. Letting $\theta = s/\sqrt{2}$ we have

$$\begin{aligned} & \underline{f \wedge \kappa\mathbf{B}} \\ &= \left(\sin\left(\frac{s}{\sqrt{2}}\right)\mathbf{e}_1 + \cos\left(\frac{s}{\sqrt{2}}\right)\mathbf{e}_2 + \frac{s}{\sqrt{2}}\mathbf{e}_3 + \mathbf{e}_0 \right) \wedge \frac{1}{2} \left(\frac{\cos\left(\frac{s}{\sqrt{2}}\right)\mathbf{e}_1 - \sin\left(\frac{s}{\sqrt{2}}\right)\mathbf{e}_2 - \mathbf{e}_3}{\sqrt{2}} \right) \\ &= \frac{1}{2\sqrt{2}} (\sin\theta\mathbf{e}_1 + \cos\theta\mathbf{e}_2 + \theta\mathbf{e}_3 + \mathbf{e}_0) \wedge (\cos\theta\mathbf{e}_1 - \sin\theta\mathbf{e}_2 - \mathbf{e}_3) \\ &= \frac{1}{2\sqrt{2}} \left(-(\sin^2\theta + \cos^2\theta)\mathbf{e}_{12} + (-\cos\theta + \theta\sin\theta)\mathbf{e}_{23} + (-\sin\theta + \theta\sin\theta)\mathbf{e}_{13} \right. \\ &\quad \left. - \cos\theta\mathbf{e}_{10} + \sin\theta\mathbf{e}_{20} + \mathbf{e}_{30} \right) \\ &= \frac{1}{2\sqrt{2}} \left(-\mathbf{e}_{12} + (-\cos\theta + \theta\sin\theta)\mathbf{e}_{23} + (-\sin\theta + \theta\sin\theta)\mathbf{e}_{13} - \cos\theta\mathbf{e}_{10} + \sin\theta\mathbf{e}_{20} + \mathbf{e}_{30} \right). \end{aligned}$$

Taking the left complement, we get

$$\begin{aligned} & \underline{f \wedge \kappa \mathbf{B}} \\ &= \frac{1}{2\sqrt{2}} \left(-\mathbf{e}_{30} + (-\cos \theta + \theta \sin \theta) \mathbf{e}_{10} + (\sin \theta - \theta \sin \theta) \mathbf{e}_{20} - \cos \theta \mathbf{e}_{23} - \sin \theta \mathbf{e}_{13} + \mathbf{e}_{12} \right). \end{aligned}$$

Combining this result with

$$\begin{aligned} r_T &= \frac{\cos \left(\frac{s}{\sqrt{2}} \right) \mathbf{e}_{10} - \sin \left(\frac{s}{\sqrt{2}} \right) \mathbf{e}_{20} + \mathbf{e}_{30}}{\sqrt{2}} \\ &= \frac{1}{2\sqrt{2}} \left(\cos \theta \mathbf{e}_{10} - \sin \theta \mathbf{e}_{20} + \mathbf{e}_{30} \right) \end{aligned}$$

we have

$$r_B = \frac{1}{2\sqrt{2}} \left(\theta \sin \theta \mathbf{e}_{10} + -\theta \sin \theta \mathbf{e}_{20} - \cos \theta \mathbf{e}_{23} - \sin \theta \mathbf{e}_{13} + \mathbf{e}_{12} \right).$$

Appendix D

Comparison of Notations

The notation in this thesis is a combination of the notation of Dorst and De Keninck [6] and Lengyel [16]. A comparison of the notation is summarized in Table D.1. Both Dorst and DeKeninck and Lengyel’s notation consider elements to have a default representation. Dorst and De Keninck’s notation considers the dual representation as the default representation of elements. Thus, in 3D PGA, vectors represent planes, 2-blades represent lines, and 3-blades represent points. Therefore, application of versors can be applied to elements as they are constructed rather than mapping to their complement. Lengyel’s notation uses the direct representation as the default. Thus, in 3D PGA, vectors represent points, 2-blades represent lines, and 3-blades represent planes. Lengyel’s notation makes use of a product called the antigeometric product \forall , which we do not detail here.

The approach to duality also differs between the two notations. Dorst and De Keninck make use the Hodge dual operator \star . The Hodge dual operator is typically only defined for geometric algebras with non-degenerate signatures [5, 7]. Such definitions cannot apply to PGA since PGA contains a basis vector which squares to 0, i.e., PGA has a degenerate signature. However, Dorst and De Keninck propose an alternative definition for the Hodge dual operator that establishes a version of the operator that is well defined for degenerate signatures. In particular,

$$E_k(\star E_k) = \mathbf{E}_k \tilde{\mathbf{E}}_k \mathcal{I},$$

Notation	Ours	Dorst and De Keninck	Lengyel
Projective axis	\mathbf{e}_0	\mathbf{e}_0	\mathbf{e}_4
Pseudoscalar	$\mathbb{1} = \mathbf{e}_{1230}$	$\mathcal{I} = \mathbf{e}_{0123}$	$\mathbb{1} = \mathbf{e}_{1234}$
Versor application	$V \underline{E} V^{-1}$	$V E V^{-1}$	$V \forall E \forall V^{-1}$
Duality	\underline{E} and \overline{E}	$\star E$ and $\star^{-1} E$	\underline{E} and \overline{E}

Table D.1: A table comparing the notation of this thesis, Dorst and De Keninck, and Lengyel.

where \mathbf{E}_k is the Euclidean part of E_k and \sim denotes reversing the element (see Dorst et al. [17] for details on the reverse operation). The factor $\mathbf{E}_k \widetilde{\mathbf{E}}_k$ has the effect of negating the element for every component basis vector of \mathbf{E}_k with a negative signature. As a result, when all of the component basis vectors of \mathbf{E}_k are non-negative (as is the case in PGA), we have $\mathbf{E}_k \widetilde{\mathbf{E}}_k = 1$ and thus

$$E_k(\star E_k) = \mathcal{I}.$$

This closely resembles the definition of the right complement

$$E_k \wedge \overline{E}_k = \mathbb{1}.$$

However, note that $\mathcal{I} \neq \mathbb{1}$. In the 3-dimensional case, we have $\mathcal{I}_3 = \mathbf{e}_{0123}$ and $\mathbb{1}_3 = \mathbf{e}_{1230}$. Generalizing to the n -dimensional case we have $\mathcal{I}_n = \mathbf{e}_{0123\dots n}$ and $\mathbb{1}_n = \mathbf{e}_{123\dots n0}$. By anticommutativity these are related by

$$\mathcal{I}_n = \mathbf{e}_{0123\dots n} = (-1)^n \mathbf{e}_{123\dots n0} = (-1)^n \mathbb{1}_n.$$

Therefore, in an n -dimensional space with only non-negative signatures, we have

$$\begin{aligned} \star A &= (-1)^n \overline{A} \\ \star^{-1} A &= (-1)^n \underline{A}. \end{aligned}$$

In 3D PGA, $n = 4$. Thus, for a vector v we have $\overline{v} = -\underline{v}$ and hence

$$\star v = \overline{v} = -\underline{v} = -\star^{-1} v$$

As an example, converting Equation 4.5 into Dorst and De Keninck's notation, we have

$$r_B = (-\star f) \vee (\mathbf{T}' \mathbf{T} \mathbf{e}_0) + \mathbf{T} \mathbf{e}_0. \quad (\text{D.1})$$

However, note that since f is of the form $f = f_{\bullet} + \mathbf{e}_0$ its default representation is not a point in Dorst and De Keninck's notation. If the parameterized curve is represented by $g := -\star f$ then

$$r_B = g \vee (\mathbf{T}' \mathbf{T} \mathbf{e}_0) + \mathbf{T} \mathbf{e}_0 \quad (\text{D.2})$$

where $\mathbf{T} = f' / \|f'\| = \star g' / \|\star g'\|$.

In this thesis, we use the left and right complement rather than the Hodge dual due to its simplicity and consistent definition throughout the literature in the degenerate case. We use \mathbf{e}_0 to represent the projective axis due to the property that $\mathbf{e}_0^2 = 0$ and to be consistent with Dorst and De Keninck. We use the pseudoscalar $\mathbb{1} = \mathbf{e}_{1230}$ so that the order of the Euclidean axes and the projective axis is consistent with Lengyel.